Figure 5. Kinetic analyses of various glucuronide formations by the single and double expression system. Zidovudine O-glucuronide formation (A–D), estradiol 3-O-glucuronide formation (E), imipramine N-glucuronide formation (F), serotonin O-glucuronide formation (G), and propofol O-glucuronide formation (H) were measured as described in Materials and Methods Section. Data are mean $\pm$ SD of three independent determinations.

Table 1. Kinetic Parameters for Zidovudine O-Glucuronidation by Single and Double Expression Systems

	K_m (μM)	V_{max} (pmol/min/U)	CL_{int} (μL/min/U)
2B7	282 ± 16	449 ± 16	1.6 ± 0.1
2B7/1A1-1	261 ± 26	$824 \pm 11^{**}$	$3.2 \pm 0.2^{**}$
2B7/1A1-2	261 ± 12	$586 \pm 23^{**}$	$2.2 \pm 0.0^{**}$
2B7/1A4-1	252 ± 14	$853 \pm 33^{**}$	$3.4 \pm 0.1^{**}$
2B7/1A4-2	$211 \pm 4^{**}$	$790 \pm 16^{**}$	$3.7 \pm 0.1^{**}$
2B7/1A6-1	$203 \pm 3^{**}$	$719 \pm 25^{**}$	$3.5 \pm 0.1^{**}$
2B7/1A6-2	$197 \pm 3^{**}$	$1090 \pm 26^{**}$	$5.5 \pm 0.1^{**}$
2B7/1A9-1	$196 \pm 12^{**}$	$820 \pm 17^{**}$	$4.2 \pm 0.2^{**}$
2B7/1A9-2	$224 \pm 28^{**}$	$943 \pm 58^{**}$	$4.2 \pm 0.3^{**}$

Data are mean $\pm$ SD of three independent determinations.
$^{**}P < 0.01$ compared with the single expression system.

observed in the double expression systems. The association between UGT2B7 and UGT1A enzymes was proven by immunoprecipitation assay. First, we used the rabbit anti-UGT2B7, rabbit or goat anti-UGT2B antibodies for the immunoprecipitation. However, these antibodies did not successfully immunoprecipitate the UGT2B7 protein (data not shown). Therefore, we used the anti-human UGT1A or anti-human UGT1AC antibodies for immunoprecipitation, which could specifically immunoprecipitate the UGT1A proteins. These antibodies coimmunoprecipitated the UGT2B7 using the double expression systems of UGT2B7/1A, supporting a previous study showing the coimmunoprecipitation of UGT2B7 and UGT1A1 or UGT1A6 using human liver microsomes.[27] When the anti-human UGT1A antibody from BD Gentest was used for immunoprecipitation, coimmunoprecipitated UGT2B7 from the double expression system of UGT2B7/1A1 was lower than those from the other double expression systems (Fig. 3A). When the anti-human UGT1AC antibody prepared by Ikushiro et al.[22] was used for immunoprecipitation, coimmunoprecipitated UGT2B7 from the double expression system of UGT2B7/1A1 and UGT2B7/1A6 was lower than those from the other double expression systems (Fig. 3B). These results may indicate that the extent of interaction with UGT2B7 might vary in

Table 2. Kinetic Parameters for Estradiol 3-O-, Imipramine N-, Serotonin O-, and Propofol O-Glucuronidations by Single and Double Expression Systems

	S_{50} (μM)	V_{max} (nmol/min/U)	n	CL_{max} (μL/min/U)
Estradiol 3-O-glucuronidation				
1A1	17.5 ± 3.3	0.8 ± 0.0	1.4 ± 0.2	27.0 ± 2.8
2B7/1A1-1	$12.6 \pm 0.3^{*}$	0.9 ± 0.1	1.7 ± 0.1	$37.0 \pm 2.9^{**}$
2B7/1A1-2	$9.9 \pm 0.5^{**}$	0.8 ± 0.1	$2.2 \pm 0.2^{**}$	$41.7 \pm 1.1^{**}$

	K_m (mM)	V_{max} (nmol/min/U)		CL_{int} (μL/min/U)
Imipramine N-glucuronidation				
1A4	0.6 ± 0.0	1.4 ± 0.1		2.3 ± 0.1
2B7/1A4-1	$2.5 \pm 0.3^{**}$	$4.3 \pm 0.8^{**}$		1.8 ± 0.5
2B7/1A4-2	$2.4 \pm 0.4^{**}$	$4.8 \pm 0.2^{**}$		2.1 ± 0.3

	K_m (mM)	V_{max} (nmol/min/U)		CL_{int} (μL/min/U)
Serotonin O-glucuronidation				
1A6	7.6 ± 2.0	2.7 ± 0.7		0.4 ± 0.1
2B7/1A6-1	5.5 ± 0.7	$4.4 \pm 0.4^{*}$		$0.8 \pm 0.1^{**}$
2B7/1A6-2	4.6 ± 0.8	$5.4 \pm 0.3^{**}$		$1.2 \pm 0.1^{**}$

	K_m (μM)	V_{max} (nmol/min/U)	K_i (mM)	CL_{int} (μL/min/U)
Propofol O-glucuronidation				
1A9	67.7 ± 5.2	43.7 ± 3.7	1.0 ± 0.1	0.7 ± 0.0
2B7/1A9-1	64.3 ± 5.4	$84.7 \pm 7.3^{**}$	1.0 ± 0.2	$1.3 \pm 0.2^{**}$
2B7/1A9-2	56.2 ± 6.0	44.4 ± 2.6	1.3 ± 0.2	0.8 ± 0.1

Data are mean $\pm$ SD of three independent determinations.
$^{*}P < 0.05$ compared with the single expression system.
$^{**}P < 0.01$ compared with the single expression system.

each UGT1A enzyme. Further validation is needed to estimate the differences in the extent of the hetero-oligomerizations of UGT2B7 and each UGT1A enzyme.

The interaction between UGT2B7 and UGT1A enzymes was supported by the thermal stability study (Fig. 4). UGT2B7 activity was decreased to 5% of control by the heat treatment at 47°C for 15 min in the presence of UDPGA. In contrast, we previously reported that UGT1A1 (60–70% of control), UGT1A4 (80–90% of control), UGT1A6 (90–95% of control), and UGT1A9 (100% of control) could retain their activities after the heat treatment.[18] These results suggest that UGT2B7 is a relatively thermally unstable enzyme. Interestingly, the coexpression of UGT1A enzymes increased the tolerability of UGT2B7. Thus, the findings support the existence of protein–protein interaction between UGT2B7 and UGT1As.

Previously, we reported that human UGT1A1, UGT1A4, UGT1A6, and UGT1A9 interact with each other changing their enzyme kinetics.[17–19] The current study found that UGT2B7 interacts with UGT1A1, UGT1A4, UGT1A6, and UGT1A9 affecting their kinetics and *vice versa* (Fig. 5). Zidovudine *O*-glucuronidation catalyzed by UGT2B7 was increased by the coexpressed UGT1A1, UGT1A4, UGT1A6, and UGT1A9. However, Kurkela et al.[21] has reported that the coexpressed UGT1A6 decreased the zidovudine *O*-glucuronidation and morphine *O*-glucuronidation catalyzed by UGT2B7. The most likely explanation for the discrepancy is that the host cells used were different in our study (HEK293 cells) and their study (Sf9 insect cells). It may be suggested that the differences in the lipid components and/or membrane circumstance may affect the interaction between UGT enzymes. Furthermore, the present study demonstrated that UGT2B7 increased the enzyme activities of UGT1A, UGT1A4, UGT1A6, and UGT1A9 when estradiol, imipramine, serotonin, and propofol were used as substrates. However, we may have to evaluate the activities using multiple substrates, since we previously found that the effects of interaction of UGT1A enzymes were dependent on the substrates.[17] A dose dependency was not observed in the effects on the kinetics between two different clones. We normalized the enzymatic activities with the protein levels determined by SDS–PAGE/immunoblot analysis. However, the detected bands at around 50 kDa would correspond to the sum of monomer and homodimer as well as heterodimer. Thus, the expression ratio of UGT2B/UGT1A may

not represent the actual content of heterodimer. This might be one of reasons for no dose dependency.

It is conceivable that all of the human UGT2B and UGT1A enzymes interact in various combinations changing their enzymatic properties. We can envisage that the interaction would occur in human liver microsomes. Usually, recombinant systems express only a single enzyme to evaluate its enzymatic properties. In the case of cytochrome P450, when multiple isoforms are involved in a given metabolic pathway, the data obtained from the recombinant enzymes can be applied to predict the contribution of each cytochrome P450 enzyme, because the activity of a certain P450 isoform is not affected by other isoforms and because we can determine the absolute expression levels of each P450 protein in human liver microsomes. This theory could not be applied for UGT because of their complicated interactions depending on the UGT isoforms, substrates, and the expression ratios of multiple UGT isoforms, even if we can determine the absolute protein expression levels of each UGT enzyme. Thus, it would be difficult to fully understand the contribution of each UGT isoform from the output activity in human liver microsomes.

In conclusion, the present study demonstrated that UGT2B7 protein interacts with UGT1A1, UGT1A4, UGT1A6, and UGT1A9 proteins. The interactions affected their enzymatic activities and resulted in altered kinetic parameters for glucuronidations. Such complicated interactions would also make difficult the prediction of *in vivo* clearance from *in vitro* data.

ACKNOWLEDGMENTS

REFERENCES

1. Dutton GJ. Acceptor substrates of UDP glucuronosyltransferase and their assay. In: Dutton GJ, editor. Glucuronidation of drugs and other compounds. Boca Raton, FL: CRC Press. 1980. pp. 69–78.
2. Mackenzie PI, Walter Bock K, Burchell B, Guillemette C, Ikushiro S, Iyanagi T, Miners JO, Owens IS, Nebert DW. 2005. Nomenclature update for the mammalian UDP glycosyltransferase (UGT) gene

superfamily. Pharmacogenet Genomics 15:677–685.

3. Ritter JK, Chen F, Sheen YY, Tran HM, Kimura S, Yeatman MT, Owens IS. 1992. A novel complex locus UGT1 encodes human bilirubin, phenol, and other UDP-glucuronosyltransferase isozymes with identical carboxyl termini. J Biol Chem 267:3257–3261.

4. Tukey RH, Strassburg CP. 2000. Human UDP-glucuronosyltransferases: Metabolism, expression and disease. Annu Rev Pharmacol Toxicol 40:581–616.

5. Fisher MB, Paine MF, Strelevitz TJ, Wrighton SA. 2001. The role of hepatic and extrahepatic UDP-glucuronosyltransferases in human drug metabolism. Drug Metab Rev 33:273–297.

6. Nakamura A, Nakajima M, Yamanaka H, Fujiwara R, Yokoi T. 2008. Expression of UGT1A and UGT2B mRNA in human normal tissues and various cell lines. Drug Metab Dispos 36:1461–1464.

7. Matern H, Matern S, Gerok W. 1982. Isolation and characterization of rat liver microsomal UDP-glucuronosyltransferase activity toward chenodeoxycholic acid and testosterone as a single form of enzyme. J Biol Chem 257:7422–7429.

8. Peters WH, Jansen PL, Nauta H. 1984. The molecular weights of UDP-glucuronosyltransferase determined with radiation-inactivation analysis. a molecular model of bilirubin UDP-glucuronyltransferase. J Biol Chem 259:11701–11705.

9. Gschaidmeier H, Bock KW. 1994. Radiation inactivation analysis of microsomal UDP-glucuronosyltransferases catalysing mono- and diglucuronide formation of 3,6-dihydroxybenzo(a)pyrene and 3,6-dihydroxychrysene. Biochem Pharmacol 48:1545–1549.

10. Ikushiro S, Emi Y, Iyanagi T. 1997. Protein-protein interactions between UDP-glucuronosyltransferase isozymes in rat hepatic microsomes. Biochemistry 36:7154–7161.

11. Meech R, Mackenzie PI. 1997. UDP-glucuronosyltransferase, the role of the amino terminus in dimerization. J Biol Chem 272:26913–26917.

12. Ghosh SS, Sappal BS, Kalpana GV, Lee SW, Chowdhury JR, Chowdhury NR. 2001. Homodimerization of human bilirubin-uridine-diphosphoglucuronate glucuronosyltransferase-1 (UGT1A1) and its functional implications. J Biol Chem 276:42108–42115.

13. Ishii Y, Miyoshi A, Watanabe R, Tsuruda K, Tsuda M, Yamaguchi-Nagamatsu Y, Yoshisue K, Tanaka M, Maji D, Ohgiya S, Oguri K. 2001. Simultaneous expression of guinea pig UDP-glucuronosyltransferase 2B21 and 2B22 in COS-7 cells enhances UDP-glucuronosyltransferase 2B21-catalyzed morphine-6-glucuronide formation. Mol Pharmacol 60:1040–1048.

14. Kurkela M, Hirvonen J, Kostiainen R, Finel M. 2004. The interactions between the N-terminal

and C-terminal domains of the human UDP-glucuronosyltransferases are partly isoform-specific and may involve both monomers. Biochem Pharmacol 68:2443–2450.

15. Kurkela M, Garcia-Horsman JA, Luukkanen L, Morsky S, Taskinen J, Baumann M, Kostiainen R, Hirvonen J, Finel M. 2003. Expression and characterization of recombinant human UDP-glucuronosyltransferases (UGTs). UGT1A9 is more resistant to detergent inhibition than the other UGTs and was purified as an active dimeric enzyme. J Biol Chem 278:3536–3544.

16. Operana TN, Tukey RH. 2007. Oligomerization of the UDP-glucuronosyltransferase 1A proteins. Homo- and heterodimerization analysis by fluorescence resonance energy transfer (FRET) and co-immunoprecipitation. J Biol Chem 282:4821–4829.

17. Fujiwara R, Nakajima M, Yamanaka H, Katoh M, Yokoi T. 2007. Interactions between human UGT1A1, UGT1A4, and UGT1A6 affect their enzymatic activities. Drug Metab Dispos 35:1781–1787.

18. Fujiwara R, Nakajima M, Yamanaka H, Nakamura A, Katoh M, Ikushiro S, Sakaki T, Yokoi T. 2007. Effects of coexpression of UGT1A9 on enzymatic activities of human UGT1A isoforms. Drug Metab Dispos 35:747–757.

19. Nakajima M, Yamanaka H, Fujiwara R, Katoh M, Yokoi T. 2007. Stereoselective glucuronidation of 5-(4′-hydroxyphenyl)-5-phenylhydantoin by human UDP-glucuronosyltransferase (UGT) 1A1, UGT1A9, and UGT2 B15: Effects of UGT-UGT interactions. Drug Metab Dispos 35:1679–1686.

20. Williams JA, Hyland R, Jones BC, Smith DA, Hurst S, Goosen TC, Peterkin V, Koup JR, Ball SE. 2004. Drug-drug interactions for UDP-glucuronosyltransferase substrates: A pharmacokinetic explanation for typically observed low exposure (AUCi/AUC) ratios. Drug Metab Dispos 32:1201–1208.

21. Kurkela M, Patana AS, Mackenzie PI, Court MH, Tate CG, Hirvonen J, Goldman A, Finel M. 2007. Interactions with other human UDP-glucuronosyltransferases attenuate the consequences of the Y485D mutation on the activity and substrate affinity of UGT1A6. Pharmacogenet Genomics 17:115–126.

22. Ikushiro S, Emi Y, Kato Y, Yamada S, Sakaki T. 2006. Monospecific antipeptide antibodies against human hepatic UDP-glucuronosyltransferase 1A subfamily (UGT1A) isoforms. Drug Metab Pharmacokinet 21:70–74.

23. Court MH, Krishnaswamy S, Hao Q, Duan SX, Patten CJ, Von Moltke LL, Greenblatt DJ. 2003. Evaluation of 3′-azido-3′-deoxythymidine, morphine, and codeine as probe substrates for UDP-glucuronosyltransferase 2B7 (UGT2B7) in human liver microsomes: Specificity and influence of the UGT2B7*2 polymorphism. Drug Metab Dispos 31:1125–1133.

24. Houston JB, Kenworthy KE. 2000. In vitro-in vivo scaling of CYP kinetic data not consistent with the classical Michaelis-Menten model. Drug Metab Dispos 28:246–254.

25. Uchaipichat V, Mackenzie PI, Guo XH, Gardner-Stephen D, Galetin A, Houston JB, Miners JO. 2004. Human UDP-glucuronosyltransferases, isoform selectivity and kinetics of 4-methylumbelliferone and 1-naphthol glucuronidation, effects of organic solvents, and inhibition by diclofenac and probenecid. Drug Metab Dispos 32:413–423.

26. Finel M, Kurkela M. 2008. The UDP-glucuronosyltransferases as oligomeric enzymes. Curr Drug Metab 9:70–76.

27. Fremont JJ, Wang RW, King CD. 2005. Coimmunoprecipitation of UDP-glucuronosyltransferase isoforms and cytochrome P450 3A4. Mol Pharmacol 67:260–262.

379

MicroRNAs Regulate Human Hepatocyte Nuclear Factor 4α, Modulating the Expression of Metabolic Enzymes and Cell Cycle[*]

Shingo Takagi[1], Miki Nakajima, Katsuhiko Kida, Yu Yamaura, Tatsuki Fukami, and Tsuyoshi Yokoi[2]

From Drug Metabolism and Toxicology, Division of Pharmaceutical Sciences, Graduate School of Medical Science, Kanazawa University, Kakuma-machi, Kanazawa 920-1192, Japan

Hepatocyte nuclear factor (HNF) 4α is a key transcription factor regulating endo/xenobiotic-metabolizing enzymes and transporters. We investigated whether microRNAs are involved in the regulation of human HNF4α. Potential recognition elements for miR-24 (MRE24) were identified in the coding region and the 3'-untranslated region (3'-UTR), and those for miR-34a (MRE34a) were identified in the 3'-UTR in HNF4α mRNA. The HNF4α protein level in HepG2 cells was markedly decreased by the overexpression of miR-24 and miR-34a. The HNF4α mRNA level was significantly decreased by the overexpression of miR-24 but not by miR-34a. In luciferase analyses in HEK293 cells, the reporter activity of plasmid containing the 3'-UTR of HNF4α was significantly decreased by miR-34a. The reporter activity of plasmid containing the HNF4α coding region downstream of the *luciferase* gene was significantly decreased by miR-24. These results suggest that the MRE24 in the coding region and MRE34a in the 3'-UTR are functional in the negative regulation by mRNA degradation and translational repression, respectively. The down-regulation of HNF4α by these microRNAs resulted in the decrease of various target genes such as cytochrome P450 7A1 and 8B1 as well as morphological changes and the decrease of the S phase population in HepG2 cells. We also clarified that the expressions of miR-24 and miR-34a were regulated by protein kinase C/mitogen-activated protein kinase and reactive oxygen species pathways, respectively. In conclusion, we found that human HNF4α was down-regulated by miR-24 and miR-34a, the expression of which are regulated by cellular stress, affecting the metabolism and cellular biology.

Human hepatocyte nuclear factor 4α (HNF4α, NR2A1),[3] which belongs to the nuclear hormone receptor superfamily,

is highly expressed in liver and regulates the expression of various genes involved in the synthesis/metabolism of fatty acid, cholesterol, glucose, and urea (1). It is well recognized that endo/xenobiotic-metabolizing enzymes such as cytochrome P450s (CYPs), UDP-glucuronosyltransferases, sulfotransferase as well as ATP-binding cassette transporters, organic anion transporters and organic cation transporters are under the control of HNF4α (2). HNF4α transactivates the expression of target genes not only via direct binding to their regulatory sequences but also through the regulation of other transcriptional factors such as pregnane X receptor and constitutive androstane receptor, which regulate these target genes. HNF4α forms large transcriptional regulatory networks in the liver. Therefore, it is believed that the change of HNF4α expression has a great impact upon the function of the liver.

Bile acids are important regulatory molecules mediating cholesterol synthesis and glucose metabolism as well as their own synthesis (3). It is well known that HNF4α positively regulates the expression of bile acid-synthesizing enzymes such as CYP7A1 and CYP8B1. When bile acids are accumulated, the HNF4α-mediated transactivation is inhibited by short heterodimer partner, which is up-regulated by bile acid-activating farnesoid X receptor (4, 5). Bile acids are known to activate the mitogen-activated protein kinase (MAPK) signaling pathway. It is known that the expression and function of HNF4α are up- or down-regulated through extracellular signal-regulated kinase (ERK), c-Jun NH$_2$-terminal kinase (JNK), and p38 MAPK pathways (6–8). In addition, chenodeoxycholic acid, a toxic bile acid, has been reported to decrease the HNF4α mRNA expression via unknown pathways (9). Thus, the bile acid synthesis would be fine-tuned through the modulation of the expression and/or activity of HNF4α. However, the regulatory mechanism of the HNF4α expression has not still been fully understood.

MicroRNAs (miRNAs) are a recently discovered family of short noncoding RNA whose final product is an ~22-nucleotide functional RNA molecule (10). They regulate the expression of target genes by binding to complementary regions of transcripts to repress their translation or mRNA degradation. At present, more than 700 miRNAs have been identified in humans. They are expressed in a cell- or tissue-specific manner. For example, miR-122 is most abundantly and specifically expressed in liver (11). It has been demonstrated that silencing

381

TABLE 1

Primers for real time RT-PCR

The nucleotide sequences of miRNAs and the others were adopted from miRBase sequences and the GenBank™ database, respectively.

Target gene	Accession No.	Forward (5′ to 3′)	Reverse (5′ to 3′)
HNF4α	NM_000457	TGTCCCGACAGATCACCTC	CACTCAACGAGAACCAGCAG
CYP7A1	NM_000780	CAGTGCCTCCCTCAACATCC	GACATATTGTAGCTCCCGATCC
CYP8B1	NM_004391	CTACACGAAGGACAAGGAGCAGGAC	GTGGCTCACGGAGAGCATCTTGTG
CYP27A1	NM_000784	GGCAACGGAGCTTAGAGGAGATTC	CATCCACATTGGACCGTACTTGGC
PEPCK	NM_002591	AGCTCGGTCGCTGGATGTCAGAG	GTAGGGTGAATCCGTCAGCTCGATG
p16	NM_000077	TGCCCAACGCACCGAATAGTTACG	TGCACGGGTCGGGTGAGAG
p21	NM_000389	CTGTCACTGTCTTGTACCCTTGTGC	GGAGAAGATCAGCCGGCGTTTG
p27	NM_004064	AGCAATGCGCAGGAATAAGGAAGCG	GTTTGACGTCTTCTGAGGCCAGG
GAPDH	NM_002046	CCAGGGCTGCTTTTAACTC	GCTCCCCCCTGCAAATGA
U6 snRNA	NR_004394	CGCTTCGGCAGCACATATACTAA	TATGGAACGCTTCACGAATTTGC
Pre-miR-24-1	MI0000080	TCCGGTGCCTACTGAGCTGATATC	CTGTTCCTGCTGAACTGAGCCA
Pre-miR-24-2	MI0000081	CGTGCCTACTGAGCTGAAACACAG	CTGTTCCTGCTGAACTGAGCCA
Pre-miR-34a	MI0000268	CCAGCTGTGAGTGTTTCTTTGGCAG	CCCACAACGTGCAGCACTTCTAG
miR-24	MIMAT0000080	TGGCTCAGTTCAGCAGGAACAG	Universal qPCR primer
miR-34a	MIMAT0000255	TGGCAGTGTCTTAGCTGGTTGT	Universal qPCR primer

of miR-122 *in vivo* causes a decrease of hepatic cholesterol biosynthesis (12). In addition, two independent studies revealed that the knockdown of all miRNAs in liver by conditional knock-out of Dicer1 resulted in apoptosis and inflammation (13) or a disruption of hepatic zonation (14). These findings indicate the physiological and biological significance of miRNAs in liver function. In this study, we examined the possibility that miRNAs might regulate the expression of human HNF4α, resulting in the modulation of liver function.

EXPERIMENTAL PROCEDURES

Chemicals and Reagents—Phorbol 12-myristate 13-acetate (PMA), H_2O_2, U0126, and SB202190 were obtained from Wako Pure Chemicals (Osaka, Japan). SP600125 was from Calbiochem. The pGL3-promoter (pGL3p) vector, pGL4.74-TK plasmid, pTARGET vector, and dual luciferase reporter assay system were purchased from Promega (Madison, WI). Lipofectamine 2000, Lipofectamine RNAiMAX, Stealth Select RNA interference for human HNF4α (HSS140902) (siHNF4α), and Negative Control Medium GC Duplex #3 (siControl) were from Invitrogen. Pre-miR miRNA precursor molecule for miR-24, miR-34a, and Negative Control #1 (Control) were from Ambion (Austin, TX). All of the primers were commercially synthesized at Hokkaido System Sciences (Sapporo, Japan). Goat anti-human HNF4α polyclonal antibodies (S-20), rabbit anti-human GAPDH polyclonal antibodies, and mouse anti-HA monoclonal antibodies were from Santa Cruz Biotechnology (Santa Cruz, CA), IMGENEX (San Diego, CA), and COVANCE (Berkeley, CA), respectively. Alexa Fluor 680 donkey anti-goat IgG was from Invitrogen. IRDye 680 goat anti-rabbit IgG and goat anti-mouse IgG were from LI-COR Biosciences (Lincoln, NE). All other chemicals and solvents were of the highest grade commercially available.

Cell Culture—The human hepatocellular carcinoma cell line HepG2 was obtained from Riken Gene Bank (Tsukuba, Japan). The human embryonic kidney cell line HEK293 was obtained from American Type Culture Collection (Manassas, VA). HepG2 cells were cultured in Dulbecco's modified Eagle's medium (Nissui Pharmaceutical, Tokyo, Japan) supplemented with 0.1 mM nonessential amino acid (Invitrogen) and 10% fetal bovine serum (Invitrogen). HEK293 cells were cultured in Dulbecco's modified Eagle's medium supplemented with 4.5 g/liter glucose, 10 mM

HEPES, and 10% fetal bovine serum. These cells were maintained at 37 °C under an atmosphere of 5% CO_2, 95% air.

Transfection of miRNAs or siRNA into HepG2 Cells—Pre-miR miRNA precursor molecule and siRNA were transfected into HepG2 cells using Lipofectamine RNAiMAX. Unless otherwise specified, the pre-miR miRNA Precursor Molecule and siRNA were transfected at final concentrations of 50 and 5 nM, respectively. After 48 h, total RNA was isolated using RNAiso according to the manufacturer's protocol. Whole cell lysates were prepared by homogenization with lysis buffer (50 mM Tris-HCl, pH 8.0, 150 mM NaCl, 1 mM EDTA, 1% Nonidet P-40) containing protease inhibitors (0.5 mM (*p*-amidinophenyl)-methanesulfonyl fluoride, 2 μg/ml aprotinin, 2 μg/ml leupeptin, 2 μg/ml pepstatin). The protein concentrations were determined using Bradford protein assay reagent (Bio-Rad) with γ-globulin as a standard.

Real Time RT-PCR for HNF4α, Its Target Genes, and miRNAs—The cDNAs were synthesized from total RNA using ReverTra Ace (Toyobo, Osaka, Japan). The primers used are shown in Table 1. The real time PCR was performed using the Mx3000P (Stratagene, La Jolla, CA) with the MxPro QPCR software as follows: after an initial denaturation at 95 °C for 2 min, the amplification was performed by denaturation at 95 °C for 15 s, annealing, and extension at 65 °C for 20 s for 40 cycles. The mRNA levels of HNF4α, phosphoenolpyruvate carboxykinase (PEPCK), p16, p21, p27, and CYPs were normalized with the GAPDH mRNA level, and the levels of pre-miR-24-1, pre-miR-24-2, pre-miR-34a, and mature miRNAs were normalized with the U6 small nuclear RNA level. For the quantification of mature miRNAs, reverse transcription was performed using the NCode miRNA first strand cDNA synthesis kit (Invitrogen) according to the manufacturer's protocol.

SDS-PAGE and Western Blot Analyses—The whole cell lysates (20 μg) were separated with 10% SDS-polyacrylamide gel electrophoresis and transferred to Immobilon-P transfer membrane (Millipore, Bedford, MA). The membranes were probed with goat anti-human HNF4α, rabbit anti-human GAPDH, or mouse anti-HA antibodies and the corresponding fluorescent dye-conjugated second antibodies. The band densities were quantified with an Odyssey infrared imaging system (LI-COR Biosciences). The HNF4α protein level was evaluated as the sum of the densities of two bands.
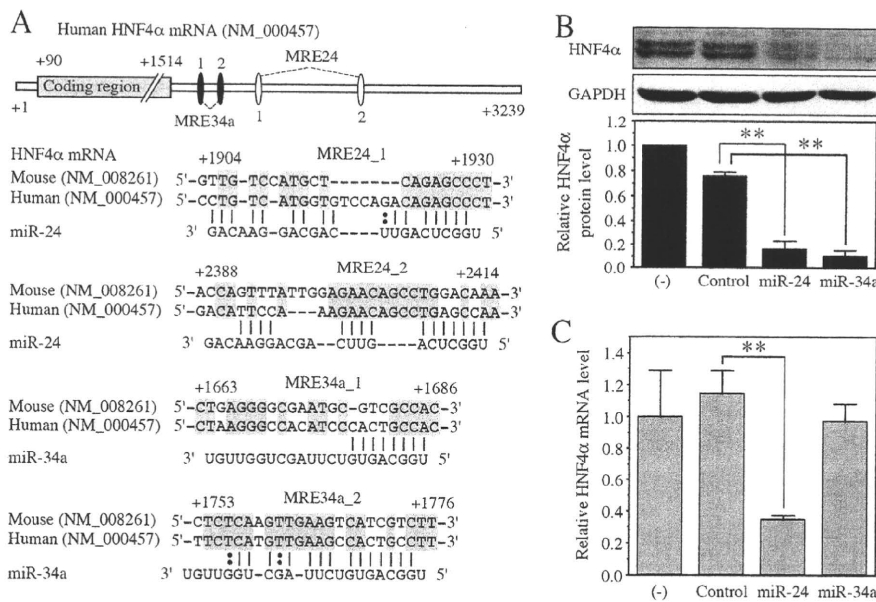
382

A

Human HNF4α mRNA (NM_000457)

HNF4α mRNA

MRE24_1

	+1904		+1930
Mouse (NM_008261)	5'-GTTG-TCCATGCT-------CAGAGCCCT-3'		
Human (NM_000457)	5'-CCTG-TC-ATGGTGTCCAGACAGAGCCCT-3'		
	||| || || || :|| |||||		
miR-24	3' GACAAG-GACGAC----UUGACUCGGU 5'		

MRE24_2

	+2388		+2414
Mouse (NM_008261)	5'-ACCAGTTTATTGGAGAACAGCCTGGACAAA-3'		
Human (NM_000457)	5'-GACATTCCA---AAGAACAGCCTGAGCCAA-3'		
miR-24	3' GACAAGGACGA--CUUG----ACUCGGU 5'		

MRE34a_1

	+1663		+1686
Mouse (NM_008261)	5'-CTGAGGGGCGAATGC-GTCGGCCAC-3'		
Human (NM_000457)	5'-CTAAGGGCCACATCCCACTGCCAC-3'		
miR-34a	3' UGUUGGUCGAUUCUGUGACGGU 5'		

MRE34a_2

	+1753		+1776
Mouse (NM_008261)	5'-CTCTCAAGTTGAAGTCATCGTCTT-3'		
Human (NM_000457)	5'-TTCTCATGTTGAAGCCACTGCCTT-3'		
	:|| |:| ||| |||||		
miR-34a	3' UGUUGGU-CGA-UUCUGUGACGGU 5'		

B

C

FIGURE 1. **The potential MREs in the 3'-UTR of HNF4α mRNA and the effects of miR-24 and miR-34a on the HNF4α level.** *A*, schematic diagrams of human HNF4α mRNA and the predicted target sites of miR-24 and miR-34a in the 3'-UTR are shown (*upper panel*). The numbering refers to the 5' end of mRNA as 1. Complementarity of miR-24 and miR-34a to the predicted target sequence of human HNF4α is shown (*lower panel*). The conserved nucleotides are highlighted in *gray boxes*. *B* and *C*, pre-miR miRNA precursor molecules were transfected into HepG2 cells at a concentration of 50 nM. After 48 h, total RNA and whole cell lysates were prepared. The HNF4α and GAPDH protein levels were determined by Western blot analyses (*B*). The HNF4α mRNA levels were determined by real time RT-PCR and normalized with the GAPDH mRNA level (*C*). The data are relative to no transfection (−). Each column represents the mean ± S.D. of three independent experiments. **, $p < 0.01$.

Construction of Plasmids—Human HNF4α cDNA including coding region and 3'-untranslated region (UTR) was amplified by PCR using cDNA prepared from HepG2 with the forward primer 5'-agaatgcgactctccaaaaccctc-3' and the reverse primer 5'-tgaattctccttaatatttatcagcaaac-3'. From this fragment, the HNF4α coding region was digested with PmaCI. These cDNA fragments were cloned into the pTARGET vector (Promega), resulting in pTARGET/HNF4α+3'-UTR and pTARGET/HNF4α plasmids. HA-tagged GFP expression plasmid was constructed by PCR using pGSU6-GFP plasmid (Genlantis, San Diego, CA) as a template with the forward primer, 5'-tttacgcgtatgtacccctacgacgtgcccgactacgccatggctagcaaaggagaagaac-3' (HA tag is underlined), and the reverse primer, 5'-tttgcggccgctcagttgtacagttcatccatgc-3'. To construct luciferase reporter plasmids, various fragments of the HNF4α coding region or 3'-UTR were inserted into the XbaI site downstream of the *luciferase* gene in the pGL3p vector. The nucleotide sequences of the constructed plasmids were confirmed by DNA sequencing analyses.

Transient Expression of HNF4α in HEK293 Cells and Transfection of miRNAs—The pTARGET/HNF4α and pTARGET/HNF4α+3'-UTR plasmids were transiently transfected with HA-tagged GFP expression plasmid and pre-miR miRNA precursor molecules into HEK293 cells. Briefly, the day before transfection, the cells were seeded into 24-well plates. After 24 h, 450 ng of the HNF4α expression plasmid, 50 ng of the pTARGET/HA-tagged GFP plasmid, and 50 nM of pre-miR miRNA precursor molecules were transfected using Lipofectamine 2000. After incubation for 48 h, the cells were harvested, and whole cell lysates were prepared as described above.

Luciferase Assay—Various luciferase reporter plasmids (pGL3p) were transiently transfected with pGL4.74-TK plasmid into HEK293 cells. Briefly, the day before transfection, the cells were seeded into 24-well plates. After 24 h, 90 ng of pGL3p plasmid, 10 ng of pGL4.74-TK plasmid, and 10 nM of pre-miR miRNA precursor molecules were transfected into HEK293 cells using Lipofectamine 2000. After incubation for 48 h, the cells were resuspended in the passive lysis buffer, and then the luciferase activity was measured with a luminometer (Wallac, Turku, Finland) using a dual luciferase reporter assay system.

Treatment of HepG2 Cells with Chemicals—HepG2 cells were seeded into 12-well plates, and after 24 h, the cells were treated with 100 nM PMA or 500 μM H_2O_2 for the indicated times. The specific inhibitors for MAPK, U0126, SB202190, and SP600125 were co-treated with PMA for 1 h or with H_2O_2 for 6 h at a final concentration of 10 μM. Total RNA was isolated as described above.

Cell Cycle Analysis—HepG2 cells were fixed with 70% ethanol at 48 h after the transfection of pre-miR miRNA precursor molecules or siRNAs. The cells were washed with FACS buffer (phosphate-buffered saline containing 0.1% bovine serum albumin) and incubated with FACS buffer containing 50 μg/ml RNase A for 30 min at 37 °C. The cells were stained with 25 μg/ml propidium iodide and analyzed using FACSCalibur and Cell Quest Pro software (BD Biosciences, San Jose, CA). Synchronization of HepG2 cells were carried out by serum deprivation. After 24 h, the cells were restimulated with serum for the indicated time.

Statistical Analysis—Statistical significance was determined by analysis of variance followed by Dunnett multiple comparisons test or Tukey method test. A value of $p < 0.05$ was considered statistically significant.

RESULTS

miR-24 and miR-34a Down-regulate HNF4α—The length of the 3'-UTR of human HNF4α is ~1.7 kb (Fig. 1*A*). Computational prediction using miRanda, PicTar, and TargetScan identified the potential recognition elements for various miRNAs including miR-1, miR-24, miR-34a, miR-326, and miR-485 in the 3'-UTR of HNF4α. Among them, we decided to investigate the effects of miR-24 and miR-34a on HNF4α expression, because they were predicted by two algorithms. Western blot analysis using whole cell lysates from HepG2 cells showed two bands of HNF4α, probably corresponding to variants 1 and 2 (Fig. 1*B*). Variant 2 is a natural splicing variant with 30 nucleo-
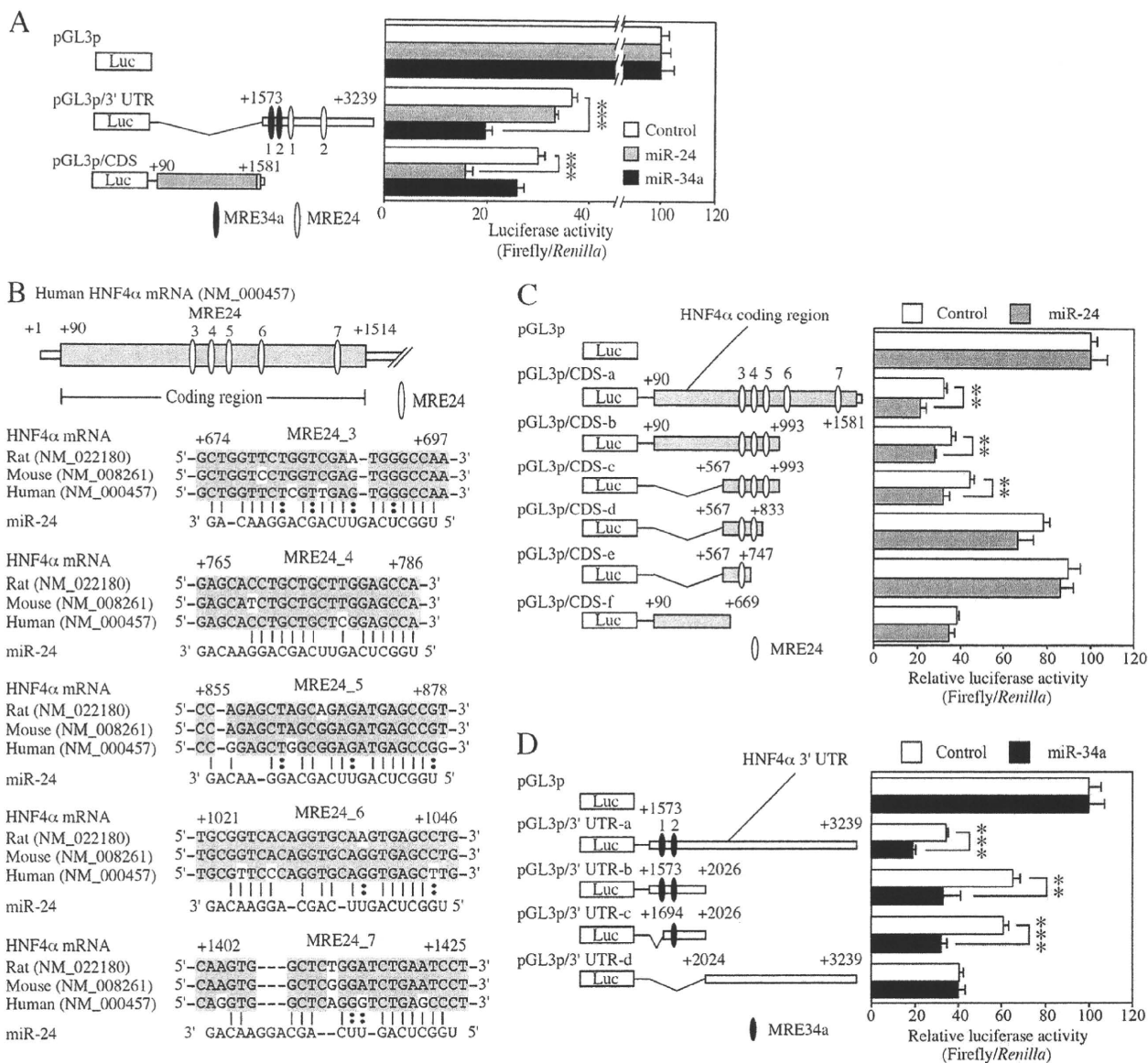
383

FIGURE 2. **Reporter analyses of MREs in the coding region and 3′-UTR of HNF4α mRNA.** *A,* reporter plasmids and pre-miR miRNA precursor molecules were co-transfected into HEK293 cells, and luciferase assays were performed after 48 h. The data were the firefly luciferase activities normalized with the *Renilla* luciferase activities relative to that of pGL3p co-transfected with each miRNA. Each column represents the mean ± S.D. of three independent experiments. ***, $p < 0.001$. *B,* schematic diagrams of the coding region of human HNF4α mRNA and mapping of predicted miR-24 target sites are described. Complementarity of miR-24 to the predicted target sequence of human HNF4α is also indicated. The conserved nucleotides are highlighted in *gray boxes*. *C* and *D,* luciferase assays were performed using plasmids containing MRE24 in the coding region (*C*) or MRE34a in the 3′-UTR (*D*) of HNF4α mRNA. The data were relative to that of pGL3p co-transfected with each miRNA. Each column represents the mean ± S.D. of three independent experiments. **, $p < 0.01$; ***, $p < 0.001$.

tides inserted in the coding region. When pre-miR miRNA precursor molecules for miR-24 and miR-34a were transfected into HepG2 cells, the mature miR-24 and miR-34a levels were increased 10.6- and 6.1-fold, respectively (data not shown). Concomitantly, the HNF4α protein levels were dramatically decreased. To investigate whether the decrease of the HNF4α protein levels was accompanied by a decrease of the mRNA levels, we determined the HNF4α mRNA levels by real time RT-PCR analysis. As shown in Fig. 1C, the HNF4α mRNA level was significantly decreased with the overexpression of miR-24, but not with miR-34a. These results suggested that miR-24 and miR-34a down-regulate the HNF4α expression by different

mechanisms, *i.e.* mRNA degradation and translational repression, respectively.

Identification of Functional MRE in Coding Region and 3′-UTR of HNF4α mRNA—In the 3′-UTR of the HNF4α mRNA, two potential miRNA recognition elements for miR-24 (MRE24_1 and MRE24_2) and miR-34a (MRE34a_1 and MRE34a_2) were predicted (Fig. 1A). To investigate whether these MRE are functional in the down-regulation of the HNF4α, luciferase assays were performed using the pGL3p/3′-UTR plasmid containing 3′-UTR of HNF4α with HEK293 cells (Fig. 2A). The luciferase activity was significantly decreased by the overexpression of miR-34a, but not by miR-24. We next
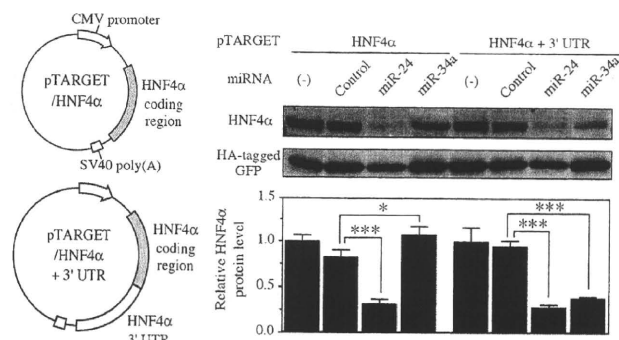
384

FIGURE 3. **Effects of miRNAs on the exogenous HNF4α expression in HEK293 cells.** The HNF4α expression plasmids including and excluding 3'-UTR used in this study are shown. These plasmids were transfected with HA-tagged GFP expression plasmid and pre-miR miRNA precursor molecules into HEK293 cells. After 48 h, whole cell lysates were prepared. The exogenously expressed HNF4α and HA-tagged GFP protein levels were determined by Western blot analyses. The data represent HNF4α protein level normalized with HA-tagged GFP level relative to that of no transfection (−). Each column represents the mean ± S.D. of three independent experiments. *, $p < 0.05$; ***, $p < 0.001$.

performed luciferase assays using the pGL3p/coding sequence (CDS) plasmid containing the coding region of HNF4α to examine the possibility that down-regulation of HNF4α by miR-24 might be mediated by elements in the coding region. The luciferase activity was significantly decreased by the overexpression of miR-24, although miR-34a did not affect the activity (Fig. 2A). These results prompted us to search for the potential recognition element of miR-24 in the coding region of HNF4α mRNA. Computational search using RNA22 identified five potential MRE24s (termed MRE24_3 to MRE24_7) in the coding region of HNF4α mRNA (Fig. 2B).

To identify the functional MREs, we performed luciferase assay using a series of deleted reporter constructs. Overexpression of miR-24 significantly decreased the luciferase activities of reporter constructs pGL3/CDS-b and pGL3/CDS-c containing MRE24_3 to _5 but did not affect the activity of the pGL3/CDS-f (Fig. 2C), indicating that three MREs would be functional. The deletion of MRE24_4 and 5 (pGL3p/CDS-d and -e) resulted in the loss of repression, suggesting that MRE24_3, 4, and 5 function cooperatively. Overexpression of miR-34a significantly decreased the activity of reporter constructs pGL3/3'-UTR-b containing MRE34a_1 and 2 but did not affect the activity of the pGL3/3'-UTR-d (Fig. 2D). The deletion of MRE34a_1 did not affect the repressive effects (pGL3p/3'-UTR-c), indicating that MRE34a_2 plays a key role in the miR-34a-mediated repression. Collectively, MRE24s in the coding region and MRE34a in the 3'-UTR of HNF4α mRNA would be functional.

miR-24 and miR-34a Act on the Coding Region and the 3'-UTR of HNF4α, Respectively—To verify that miR-24 and miR-34a act on the coding region and the 3'-UTR of HNF4α, respectively, we constructed expression systems of HNF4α that excluded or included the 3'-UTR. In the HEK293 cells transfected with pTARGET/HNF4α plasmid, the HNF4α protein level was significantly decreased by the overexpression of miR-24, but not by miR-34a (Fig. 3). In the HEK293 cells transfected with pTARGET/HNF4α+3'-UTR plasmid, the HNF4α protein level was significantly decreased by both miR-24 and miR-34a.

These results support that miR-24 and miR-34a down-regulate the HNF4α expression through recognizing the elements in the coding region and the 3'-UTR of HNF4α mRNA, respectively.

Regulation of miR-24 and miR-34a Expression—The mature miR-24 is produced from two precursors, pre-miR-24-1 and pre-miR-24-2, the genes of which are located on chromosome 9q22.32 and 19p13.12, respectively. The mature miR-34a is produced from a precursor pre-miR-34a, the gene of which is located on chromosome 1p36.22. Because the HNF4α expression and/or activity are changed in response to signals derived from bile acids, we examined whether bile acids affect the expression of miR-24 and miR-34a. First, we examined the effect of chenodeoxycholic acid on the expression of the precursors of miR-24 and miR-34a. We found that the treatment with chenodeoxycholic acid increased the pre-miR-24-2 level in HepG2 cells (3.4-fold) at a concentration of 200 μM (data not shown). Bile acids are known to activate protein kinase C (PKC) and reactive oxygen species (ROS) generation. We next investigated the effects of PKC activator PMA and ROS generator H_2O_2 on the expression of the precursors of miR-24 and miR-34a. The treatment with PMA for 0.5–3 h markedly increased the expression of the pre-miR-24-2 level (Fig. 4A). The treatment with H_2O_2 for a relatively longer time greatly increased the expression levels of pre-miR-24-2 and pre-miR-34a (Fig. 4B). This was accompanied by increases of the mature miR-24 and miR-34a levels (Fig. 4C). Interestingly, the HNF4α protein levels were significantly decreased (Fig. 4D). It was considered that PMA or H_2O_2 repressed the HNF4α expression though increasing the miR-24 and miR-34a levels.

PKC activates MAPK pathway including ERK, JNK, and p38. The PMA-dependent induction of pre-miR-24-2 was decreased by co-treatment with MAPK/ERK kinase (MEK) inhibitor U0126 or p38 inhibitor SB202190 but not with JNK inhibitor SP600125 (Fig. 4E). In contrast, these MAPK inhibitors did not affect the H_2O_2-dependent induction of pre-miR-34a (Fig. 4F). These results suggest that the ERK and p38 MAPK pathways modulate the pre-miR-24-2 level. The decrease of the HNF4α expression via activation of MAPK or generation of ROS might partly be explained by the induction of miRNAs repressing HNF4α.

miR-24- and miR-34a-dependent Down-regulation of HNF4α Decreases the Expression of Target Genes—We next investigated the effects of the miRNA-dependent down-regulation of HNF4α on the expression of target genes (Fig. 5A). The overexpression of miR-24 and miR-34a drastically decreased the CYP7A1 mRNA level in HepG2 cells. In addition, the overexpression of miR-24 and miR-34a significantly decreased the CYP8B1, CYP27A1, and PEPCK mRNA levels. To investigate whether the decrease of these mRNAs resulted from the decrease of the HNF4α protein level but not the direct effects of miRNAs, we introduced siHNF4α into the HepG2 cells. It was clearly demonstrated that the HNF4α protein level was remarkably decreased by the transfection of siHNF4α (Fig. 5B). Under this condition, the mRNA levels of CYP7A1, CYP8B1, CYP27A1, and PEPCK were significantly decreased. These results suggest that the decrease of HNF4α by miR-24 and miR-34a caused the decrease of the expression of the target genes. Because they are key enzymes for the bile acid biosynthetic
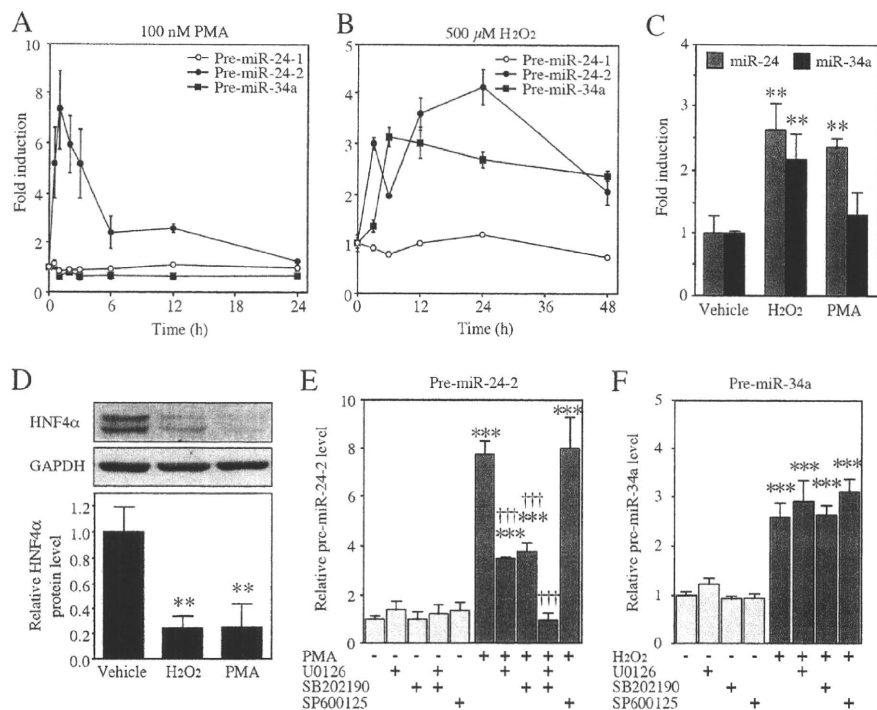
385

FIGURE 4. **Regulation of miR-24 and miR-34a through MAPK and ROS pathway, respectively.** *A* and *B*, HepG2 cells were treated with 100 nM PMA (*A*) or 500 μM H_2O_2 (*B*) for the indicated time. The pre-miRNA levels were determined by real time RT-PCR and normalized with the U6 small nuclear RNA level. The data are shown as fold changes compared with vehicle. Each point represents the mean ± S.D. of three independent experiments. *C* and *D*, HepG2 cells were treated with 100 nM PMA or 500 μM H_2O_2 for 48 h. The mature miR-24 and miR-34a levels were determined by real time RT-PCR and normalized with the U6 small nuclear RNA level (*C*). The HNF4α and GAPDH protein levels were determined by Western blot analyses (*D*). The data are relative to vehicle. Each column represents the mean ± S.D. of three independent experiments. **, $p < 0.01$, compared with vehicle. *E* and *F*, cells were co-treated with 100 nM PMA and 10 μM MAPK inhibitors for 1 h (*E*) or co-treated with 500 μM H_2O_2 and 10 μM MAPK inhibitors for 6 h (*F*). Each column represents the mean ± S.D. of three independent experiments. ***, $p < 0.001$, compared with nontreatment; †††, $p < 0.001$, compared with PMA-treated.
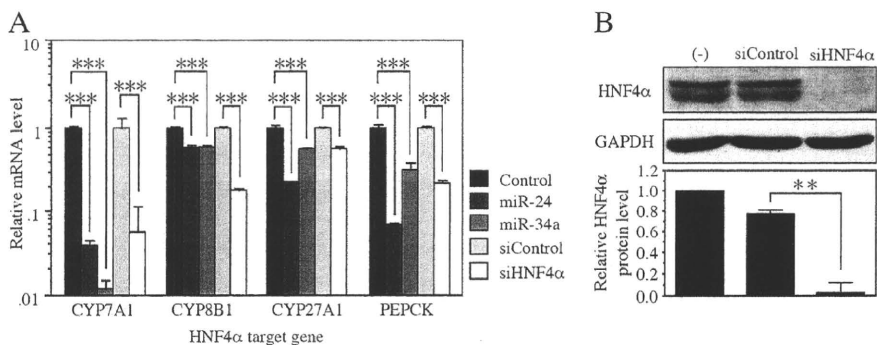

FIGURE 5. **Down-regulation of various HNF4α target genes by miR-24 and miR-34a as well as siHNF4α.** *A*, the mRNA levels of various targets of HNF4α in HepG2 cells were examined by real time RT-PCR and normalized with the GAPDH mRNA level. The data are relative to that transfected with control or siControl. Each column represents the mean ± S.D. of three independent experiments. ***, $p < 0.001$. *B*, the HNF4α and GAPDH protein levels in HepG2 cells were determined by Western blot analyses. The data are relative to no transfection (−). Each column represents the mean ± S.D. of three independent experiments. **, $p < 0.01$.

pathway and rate-limiting for gluconeogenesis, miR-24 and miR-34a may affect the hepatic functions through the regulation of HNF4α.

miR-24- and miR-34a-dependent Down-regulation of HNF4α Is Associated with Changes of Morphology and Cell Cycle Population—When miR-24 and miR-34a were overexpressed in the HepG2 cells, we noticed morphological changes including scattering and enlargement of the cells (Fig. 6*A*). Such

morphological changes were also observed when the siHNF4α was transfected. It has been reported that HNF4α is involved in the control of differentiation, cell adhesion, and cell proliferation (15–17). We investigated the effects of overexpression of miR-24 and miR-34a on the cell cycle. The percentage of S phase cells was significantly decreased by the transfection with miR-24 or miR-34a into the HepG2 cells (Fig. 6*B*). The decrease was also observed by the transfection of siHNF4α. In addition, it was found that the transfection with miR-24 or miR-34a significantly induced the mRNA level of cyclin-dependent kinase inhibitor p21 (Fig. 6*C*), although there was no clear induction of p16 and p27. The induction of p21 and p16 was also observed when the siHNF4α was transfected. These results suggest that the changes of morphology and cell population by miR-24 and miR-34a might partly be due to the down-regulation of HNF4α. However, the transfection of siHNF4α did not cause cell cycle arrest at the G_1/S transition, although the overexpression of miR-24 and miR-34a caused complete arrest at the G_1/S transition, when the cells were synchronized by serum starvation (Fig. 6*D*). Thus, miR-24 and miR-34a may arrest the cell cycle through other mechanisms that are independent of HNF4α.

DISCUSSION

HNF4α is highly expressed in liver, although it is also expressed in extrahepatic tissues such as kidney, intestine, and pancreas (1). It is constitutively active and generally acts as a positive transcriptional regulator of the expression of various transcriptional factors and enzymes. It has been reported that knock-out of HNF4α disrupts the hepatic architecture and function (15). Mutations in HNF4α are a cause of type 1 maturity onset diabetes of the young, which is the monogenic form of diabetes that results from functional defects in islet β cells (18). Thus, HNF4α is critical for tissue development and for the maintenance of a number of metabolic pathways. In this study, we investigated the role of miRNAs in the regulation of HNF4α expression.
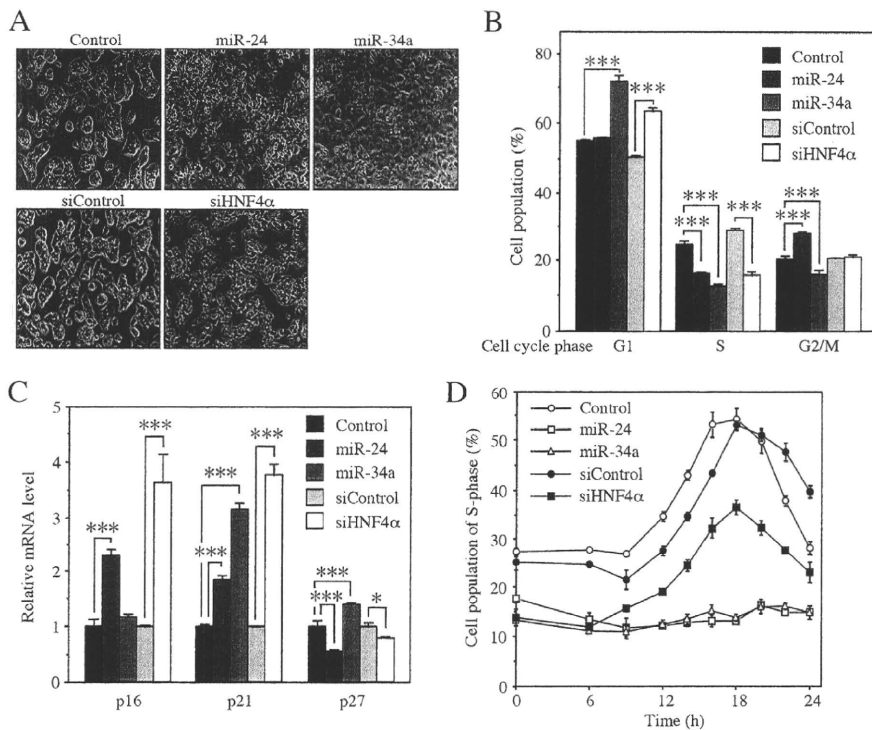
386

FIGURE 6. **Inhibition of G_1/S transition by miR-24 and miR-34a in HepG2 cells.** *A*, morphological change of HepG2 cells at 72 h after the transfection with pre-miRNA precursor molecules or siRNAs was visualized and photographed under a light microscope. *B*, cells were collected at 48 h after the transfection, and the cell population in each phase of cell cycle was analyzed by FACS. Each column represents the mean ± S.D. of three independent experiments. ***, $p < 0.001$. *C*, the p16, p21, and p27 mRNA levels were determined by real time RT-PCR and were normalized with the GAPDH mRNA level. The data are relative to that transfected with the control or siControl. Each column represents the mean ± S.D. of three independent experiments. *, $p < 0.05$; ***, $p < 0.001$. *D*, the time-dependent change of the percentages of cell population under S phase are shown. Twenty-four hours after the transfection with pre-miRNA precursor molecules or siRNAs, the cells were synchronized by serum deprivation for 24 h. Then the cells were restimulated with serum for the indicated time. Each point represents the mean ± S.D. of three independent experiments.

We found that both miR-24 and miR-34a negatively regulate the HNF4α expression. Generally, in vertebrates, miRNAs are believed to recognize elements in the 3′-UTR to repress the translation or to degrade mRNA. In this study, however, we found that the functional MREs for miR-24-dependent regulation are located in the coding region of HNF4α mRNA. This was not surprising because for other targets, it has been demonstrated the miRNA regulates through the coding region or 5′-UTR (19–21). miR-24 decreased the HNF4α mRNA level in addition to the protein level, suggesting that miR-24 is likely to repress the HNF4α expression through mRNA degradation rather than through translational repression. On the other hand, the functional MRE for miR-34a-dependent regulation is located in the 3′-UTR. miR-34a is likely to repress the HNF4α expression through translational repression, because it did not decrease the mRNA levels, although it did decrease the HNF4α protein level. Thus, it was considered that miR-24 and miR-34a regulate the human HNF4α expression through different mechanisms.

We found that the pre-miR-24-2 level was strongly increased by the treatment with PKC/MAPK activator PMA and ROS generator H_2O_2 in HepG2 cells. The activation of the PKC pathway induces cholestasis (22). The ROS pathway plays an important role in the pathogenesis of nonalcoholic steato-

hepatitis (23). Because the increase of the pre-miR-24-2 resulted in the increase of the mature miR-24 level, the mature miR-24 expression seems to be induced in these pathological conditions. Additionally, it has been reported that transforming growth factor-β, which is associated with fibrosis, increased the miR-24 level (24). Regarding HNF4α, it has been reported that cholestasis, hepatic steatosis, and fibrosis down-regulate the expression (25–27). Thus, the down-regulation of HNF4α in these diseases might be due to the induction of miR-24.

Previous studies revealed that miR-34a is regulated by p53, a tumor suppressor gene (28, 29). The present study demonstrated that the pre-miR-34a level was increased by the treatment with H_2O_2. The treatment with MAPK inhibitors failed to inhibit the induction of pre-miR-34a. ROS is known to activate p53 pathway, suggesting that the increase of pre-miR-34a might result from the p53 activation, but not MAPK pathways. It is known that chenodeoxycholic acid activates the PKC pathway and generates ROS, but it failed to increase the pre-miR-34a level in our study (data not shown). Although the reason for the discrepancy is unknown, it is surmised that miR-34a may be up-regulated directly by bile acids.

We found that the changes of morphology and cell population by miR-24 and miR-34a might be partly due to the down-regulation of HNF4α. However, detailed examination of the cell population revealed that cell cycle arrest might be caused by additional roles for miR-24 and miR-34a with other targets besides HNF4α. In fact, miR-34a is known to suppress cell cycle regulatory genes such as cyclin E2 and cyclin-dependent kinase 4, resulting in cell cycle arrest in the G_1 phase (30). Meanwhile, miR-24 has been reported to promote the proliferation of transforming growth factor-β-treated HuH7 hepatocellular carcinoma cells (24) as well as A549 lung carcinoma cells (31). These findings might be consistent with a report showing that miR-24 suppressed the translation of p16, which arrests cells in the G_1 phase (32). In contrast, Cheng *et al.* (31) have reported that miR-24 attenuated the proliferation in HeLa cells. Thus, miR-24 might function differently in different cells. In contrast to a previous study (33), the decrease of HNF4α by the transfection with siHNF4α resulted in the up-regulation of p21 gene expression. Because c-Myc interacts with HNF4α and blocks the activation of p21 promoter, the conflicting result might be due to the difference in the balance between c-Myc and HNF4α expression. Taken together, miR-24 and miR-34a would cause
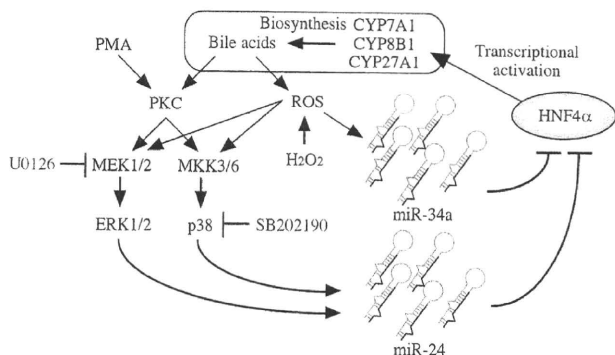
387

MicroRNA Regulates Human HNF4α

FIGURE 7. **A proposal of the regulatory loop of miR-24, miR-34a, and HNF4α in bile acid synthesis.** Bile acids are known to activate PKC and ROS generation, resulting in the activation of MAPK pathway. The miR-24 and miR-34a expression are induced by MAPK-dependent and -independent pathways, respectively. In turn, miR-24 and miR-34a negatively regulate the HNF4α. The down-regulation of HNF4α decreases the expression of bile acid-synthesizing enzymes CYP7A1 and CYP8B1, resulting in the decrease of bile acids.

cell arrest through the regulation of multiple targets in global network for cell cycle.

Of particular interest in our findings was that the miR-24- and miR-34a-dependent down-regulation of HNF4α resulted in decreases of the downstream genes. CYP7A1 catalyzes the first and rate-limiting step in the classical bile acid synthetic pathway (34). It is considered that the induction of miR-24 and miR-34a would result in decreased bile acid synthesis. In addition, gluconeogenic enzyme PEPCK was also down-regulated by the decrease of the HNF4α expression by miRNAs. Thus, miR-24 and miR-34a might affect the various hepatic functions through the negative regulation of HNF4α expression. Interestingly, we found that these miRNAs were induced by PKC/MAPK activator or ROS generator. Therefore, we propose a novel feedback regulation of bile acids synthesis (Fig. 7). Namely, bile acids activate PKC/MAPK and ROS pathways. The PKC/MAPK and ROS pathways increase the miR-24 and miR-34a expression, respectively. These miRNAs down-regulate the HNF4α expression. Accordingly, the expression of bile acid-synthesizing enzymes is decreased. Thus, we could provide new insight into the negative feedback regulation of bile acids synthesis.

In summary, we found that miR-24 and miR-34a regulate human HNF4α expression, resulting in the decrease of various downstream genes and aberrant cell cycle. Because these miRNAs are under the control of cellular stress, the miRNAs-dependent regulation of human HNF4α might contribute to pathology in liver.

REFERENCES

1. Gonzalez, F. J. (2008) *Drug Metab. Pharmacokinet.* **23,** 2–7
2. Kamiyama, Y., Matsubara, T., Yoshinari, K., Nagata, K., Kamimura, H., and Yamazoe, Y. (2007) *Drug Metab. Pharmacokinet.* **22,** 287–298
3. Hylemon, P. B., Zhou, H., Pandak, W. M., Ren, S., Gil, G., and Dent, P. (2009) *J. Lipid Res.* **50,** 1509–1520
4. Goodwin, B., Jones, S. A., Price, R. R., Watson, M. A., McKee, D. D.,

Moore, L. B., Galardi, C., Wilson, J. G., Lewis, M. C., Roth, M. E., Maloney, P. R., Willson, T. M., and Kliewer, S. A. (2000) *Mol. Cell* **6,** 517–526
5. Lee, Y. K., Dell, H., Dowhan, D. H., Hadzopoulou-Cladaras, M., and Moore, D. D. (2000) *Mol. Cell. Biol.* **20,** 187–195
6. Hatzis, P., Kyrmizi, I., and Talianidis, I. (2006) *Mol. Cell. Biol.* **26,** 7017–7029
7. Li, T., Jahan, A., and Chiang, J. Y. (2006) *Hepatology* **43,** 1202–1210
8. Guo, H., Gao, C., Mi, Z., Wai, P. Y., and Kuo, P. C. (2006) *Biochem. J.* **394,** 379–387
9. Popowski, K., Eloranta, J. J., Saborowski, M., Fried, M., Meier, P. J., and Kullak-Ublick, G. A. (2005) *Mol. Pharmacol.* **67,** 1629–1638
10. Bartel, D. P. (2004) *Cell* **116,** 281–297
11. Chang, J., Nicolas, E., Marks, D., Sander, C., Lerro, A., Buendia, M. A., Xu, C., Mason, W. S., Moloshok, T., Bort, R., Zaret, K. S., and Taylor, J. M. (2004) *RNA Biol.* **1,** 106–113
12. Krützfeldt, J., Rajewsky, N., Braich, R., Rajeev, K. G., Tuschl, T., Manoharan, M., and Stoffel, M. (2005) *Nature* **438,** 685–689
13. Hand, N. J., Master, Z. R., Le Lay, J., and Friedman, J. R. (2009) *Hepatology* **49,** 618–626
14. Sekine, S., Ogawa, R., Mcmanus, M. T., Kanai, Y., and Hebrok, M. (2009) *J. Pathol.* **219,** 365–372
15. Parviz, F., Matullo, C., Garrison, W. D., Savatski, L., Adamson, J. W., Ning, G., Kaestner, K. H., Rossi, J. M., Zaret, K. S., and Duncan, S. A. (2003) *Nat. Genet.* **34,** 292–296
16. Battle, M. A., Konopka, G., Parviz, F., Gaggl, A. L., Yang, C., Sladek, F. M., and Duncan, S. A. (2006) *Proc. Natl. Acad. Sci. U.S.A.* **103,** 8419–8424
17. Erdmann, S., Senkel, S., Arndt, T., Lucas, B., Lausen, J., Klein-Hitpass, L., Ryffel, G. U., and Thomas, H. (2007) *Biol. Chem.* **388,** 91–106
18. Stanger, B. Z. (2008) *Diabetes* **57,** 1461–1462
19. Forman, J. J., Legesse-Miller, A., and Coller, H. A. (2008) *Proc. Natl. Acad. Sci. U.S.A.* **105,** 14879–14884
20. Tay, Y., Zhang, J., Thomson, A. M., Lim, B., and Rigoutsos, I. (2008) *Nature* **455,** 1124–1128
21. Lytle, J. R., Yario, T. A., and Steitz, J. A. (2007) *Proc. Natl. Acad. Sci. U.S.A.* **104,** 9667–9672
22. Kubitz, R., Saha, N., Kühlkamp, T., Dutta, S., vom Dahl, S., Wettstein, M., and Häussinger, D. (2004) *J. Biol. Chem.* **279,** 10323–10330
23. Day, C. P. (2002) *Gut* **50,** 585–588
24. Huang, S., He, X., Ding, J., Liang, L., Zhao, Y., Zhang, Z., Yao, X., Pan, Z., Zhang, P., Li, J., Wan, D., and Gu, J. (2008) *Int. J. Cancer* **123,** 972–978
25. Geier, A., Zollner, G., Dietrich, C. G., Wagner, M., Fickert, P., Denk, H., van Rooijen, N., Matern, S., Gartung, C., and Trauner, M. (2005) *Hepatology* **41,** 470–477
26. Xie, X., Liao, H., Dang, H., Pang, W., Guan, Y., Wang, X., Shyy, J. Y., Zhu, Y., and Sladek, F. M. (2009) *Mol. Endocrinol.* **23,** 434–443
27. Yue, H. Y., Yin, C., Hou, J. L., Zeng, X., Chen, Y. X., Zhong, W., Hu, P. F., Deng, X., Zhang, J. P., Ning, B. F., Shi, J., Zhang, X., Lin, Y., and Xie, W. F. (2009) *Gut*, in press
28. Raver-Shapira, N., Marciano, E., Meiri, E., Spector, Y., Rosenfeld, N., Moskovits, N., Bentwich, Z., and Oren, M. (2007) *Mol. Cell* **26,** 731–743
29. Chang, T. C., Wentzel, E. A., Kent, O. A., Ramachandran, K., Mullendore, M., Lee, K. H., Feldmann, G., Yamakuchi, M., Ferlito, M., Lowenstein, C. J., Arking, D. E., Beer, M. A., Maitra, A., and Mendell, J. T. (2007) *Mol. Cell* **26,** 745–752
30. He, L., He, X., Lim, L. P., de Stanchina, E., Xuan, Z., Liang, Y., Xue, W., Zender, L., Magnus, J., Ridzon, D., Jackson, A. L., Linsley, P. S., Chen, C., Lowe, S. W., Cleary, M. A., and Hannon, G. J. (2007) *Nature* **447,** 1130–1134
31. Cheng, A. M., Byrom, M. W., Shelton, J., and Ford, L. P. (2005) *Nucleic Acids Res.* **33,** 1290–1297
32. Lal, A., Kim, H. H., Abdelmohsen, K., Kuwano, Y., Pullmann, R., Jr., Srikantan, S., Subrahmanyam, R., Martindale, J. L., Yang, X., Ahmed, F., Navarro, F., Dykxhoorn, D., Lieberman, J., and Gorospe, M. (2008) *PLoS One* **3,** e1864
33. Hwang-Verslues, W. W., and Sladek, F. M. (2008) *Mol. Endocrinol.* **22,** 78–90
34. Pikuleva, I. A. (2006) *Pharmacol. Ther.* **112,** 761–773

388
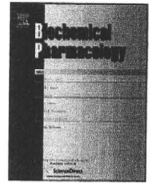
Human CYP2A6 is regulated by nuclear factor-erythroid 2 related factor 2

Shin-ichi Yokota, Eriko Higashi, Tatsuki Fukami, Tsuyoshi Yokoi, Miki Nakajima *

Drug Metabolism and Toxicology, Faculty of Pharmaceutical Sciences, Kanazawa University, Kakuma-machi, Kanazawa 920-1192, Japan

ARTICLE INFO

ABSTRACT

Human CYP2A6 is responsible for the metabolism of nicotine and coumarin as well as the metabolic activation of tobacco-related nitrosamines. Earlier studies revealed that CYP2A6 activity was increased by dietary cadmium or cruciferous vegetables, but the underlying mechanisms remain to be clarified. In the present study, we investigated the possibility that Nrf2 might be involved in the regulation of CYP2A6. Real-time RT-PCR analysis revealed that the CYP2A6 mRNA level in human hepatocytes was significantly ($P < 0.01$, 1.4-fold) induced by 10 μM sulforaphane (SFN), a typical activator of Nrf2. A computer-based search identified three putative antioxidant response elements (AREs) in the 5'-flanking region of the CYP2A6 gene at positions -1212, -2444, and -3441, termed ARE1, ARE2, and ARE3, respectively. Electrophoretic mobility shift assays demonstrated that Nrf2 bound only to ARE1. Luciferase assays using HepG2 cells revealed that the overexpression of Nrf2 significantly increased the reporter activities of the constructs containing a 30-bp fragment that included ARE1. However, the activity of the construct containing the intact 5'-flanking region (-1 to -1395) including ARE1 was not increased by the overexpression of Nrf2. In contrast, when the reporter construct was injected into mice via the tail vein, the reporter activity in the liver was significantly ($P < 0.05$, 1.9-fold) increased by SFN (1 mg/head) administration. In conclusion, we found that human CYP2A6 is regulated via Nrf2, suggesting that CYP2A6 is induced under oxidative stress.

© 2010 Elsevier Inc. All rights reserved.

1. Introduction

Human cytochrome P450 2A6 (CYP2A6), which was first purified as coumarin 7-hydroxylase [1], is a major enzyme responsible for the metabolism of nicotine [2] and cotinine [3]. CYP2A6 also metabolically activates tobacco-specific nitrosamines such as 4-methylnitrosoamino-1-(3-pyridyl)-1-butanone and N-nitrosonornicotine [4]. Many studies have suggested that the interindividual variability in CYP2A6 activity affects smoking behavior or cancer susceptibility [5–7]. Genetic polymorphisms are the major factor contributing to the interindividual differences in CYP2A6 activity and expression, but dietary or environmental factors as well as endogenous factors such as steroid hormones are also involved. To understand the regulators of CYP2A6 expression, we have studied transcriptional factors regulating CYP2A6 expression and found that pregnane X receptor [8] and estrogen receptor [9] are involved in the CYP2A6 regulation. In addition, a recent study reported the involvement of glucocorticoid receptor in the regulation of CYP2A6 [10].

It has been reported that cadmium ingestion increased the CYP2A6 expression based on the fact that the extent of urinary excretion of cadmium was positively correlated with the extent of urinary excretion of 7-hydroxycoumarin after the administration of coumarin [11]. Mouse Cyp2a5, an orthologue of human CYP2A6, has also been reported to be induced by the administration of cadmium. Abu-Bakar et al. [12] suggested that the induction of Cyp2a5 would be mediated by nuclear factor-erythroid 2 related factor 2 (Nrf2) because the induction was not observed in Nrf2 knock-out mice. Nrf2 is a transcription factor which regulates the expression of antioxidative and cytoprotective genes. Under normal conditions, Nrf2 is sequestered in the cytoplasm by Kelch-like ECH-associated protein 1, which stimulates proteasomal degradation of Nrf2 [13]. On cellular stimulation by oxidative stress, Nrf2 is dissociated from Keap1 and accumulates in the nucleus to regulate the expression of antioxidative and cytoprotective genes. Sulforaphane, which is well known as an activator of Nrf2, is contained in cruciferous vegetables such as broccoli sprouts. Interestingly, it has been reported that CYP2A6 activity was significantly increased after the consumption of broccoli (500 g/day for 6 days) by 1.4- to 5.5-fold [14]. This background prompted us to investigate whether Nrf2 might be involved in the regulation of human CYP2A6.

2. Materials and methods

2.1. Chemicals and reagents

L-Sulforaphane (SFN) and tert-butylhydroquinone (tBHQ) were obtained from LKT Laboratory (St. Paul, MN) and Wako Pure

---

Chemical Industries (Osaka, Japan), respectively. Anti-human Nrf2 antibodies (C-20) and (H-300), which recognize the C-terminus and N-terminus of the Nrf2 protein, respectively, and normal rabbit IgG were purchased from Santa Cruz Biotechnology (Santa Cruz, CA). Dual Luciferase Reporter Assay System, pGL3-basic, phRL-TK, and pGL4.74 plasmid were purchased from Promega (Madison, WI). QIAGEN Plasmid Midi kit was from QIAGEN (Valencia, CA). MiraCLEAN Endotoxin Removal Kit and TransIT-QR Hydrodynamic Delivery Solution were from Mirus Bio (Madison, WI). Oligonucleotides were commercially synthesized at Hokkaido System Sciences (Sapporo, Japan). Restriction enzymes were purchased from Takara (Shiga, Japan), TOYOBO (Osaka, Japan), and New England Biolabs (Beverly, MA). All other reagents were of the highest grade commercially available.

2.2. Cell culture

Human cryopreserved hepatocytes, lot 82 (Hispanic, female, 23 years) were purchased from In Vitro Technologies (Baltimore, MD). The hepatocytes were seeded into collagen-coated 6-well plates at 0.9×10^5 cells/well and maintained in HCM hepatocyte culture medium (Cambrex, East Rutherford, NJ) at 37 °C under 5% CO_2. After 24 h, the culture medium was changed to HCM medium (epidermal growth factor- and antibiotics-free) containing 10 μM SFN or 0.1% (v/v) DMSO vehicle. Hepatocytes were maintained for 12 h or 24 h until harvesting.

Human hepatoma cell line HepG2 was obtained from American Type Culture Collection (Manassas, VA). HepG2 cells were cultured in Dulbecco's modified Eagle's medium (DMEM) (Nissui Pharmaceutical, Tokyo, Japan) supplemented with 10% fetal bovine serum (FBS) (Invitrogen, Carlsbad, CA) and 0.1 mM nonessential amino acids (Invitrogen) at 37 °C under 5% CO_2.

2.3. Real-time RT-PCR analyses

Total RNA was isolated from human hepatocytes or mouse liver using RNAiso (Takara) following the manufacturer's protocol, and cDNA was synthesized as described previously [15]. The primers for human CYP2A6 [15] and human GAPDH [16] were described previously. The forward and reverse primers for mouse NAD(P)H:-quinone oxidoreductase 1 (NQO1) were 5′-CCCTGATTGTACTGGCC-CATT-3′ and 5′-CGTCCTTCCTTATATGCTAG-3′, respectively. The forward and reverse primers for mouse GAPDH were 5′-AAATGGGGTGAGGCCGGT-3′ and 5′-ATTGCTGACAATCTTGAGTGA-3′, respectively. Real-time RT-PCR assays were performed using the Smart Cycler (Cepheid, Sunnyvale, CA) as described previously [17].

2.4. Electrophoretic mobility shift assays

Double-stranded oligonucleotides were labeled with [γ-^{32}P] ATP using T4 polynucleotide kinase (TOYOBO) and purified by Microspin G-50 columns (GE Healthcare, Buckinghamshire, UK). The oligonucleotide sequences for ARE1 and consensus ARE (cARE) on Mus musculus heme oxygenase-1 (HO-1) promoter were 5′-GTAG-TAGCCCCTGACAAAGCAGGAATCAT-3′ and 5′-GATCTTTTATGCT-GAGTCATGGTTT-3′, respectively [18]. The labeled probe (80 fmol, ~13,000 cpm) was applied to each binding reaction in 25 mM HEPES-KOH (pH 7.9), 0.5 mM EDTA, 10% glycerol, 50 mM KCl, 0.5 mM dithiothreitol, 0.5 mM (p-amidinophenyl) methanesulfonyl fluoride, 1 μg of poly (dI-dC), 10 μg of salmon sperm DNA, and 8 μg of the nuclear extracts from 80 μM tBHQ-treated HepG2 cells with a final reaction volume of 15 μl. To determine the specificity of the binding to the oligonucleotides, competition experiments were conducted by co-incubation with 10-, 50-, and 200-fold excesses of unlabeled competitors. For super-shift experiments, 2 μg of anti-Nrf2 antibodies or normal rabbit IgG were pre-incubated with the

nuclear protein on ice for 30 min. The reactions were incubated on ice for 15 min and then loaded on 4% acrylamide gel in 0.5 × Tris-borate EDTA buffer. The gels were dried and exposed to imaging plate for 18 h. The DNA-protein complexes were detected with a Fuji Bio-Imaging Analyzer BAS 1000 (Fuji Film, Tokyo, Japan).

2.5. Human Nrf2 expression plasmid and reporter constructs

Human Nrf2 expression plasmid and the pGL3-cARE plasmid containing two copies of the cARE on the human NQO-1 gene were previously constructed [17]. Double-stranded oligonucleotide ARE1 on the human CYP2A6 gene (5′-GTAGTAGCCCCTGA-CAAAGCAGGAATCAT-3′) was cloned into the pGL3-tk plasmid digested with Sma I, resulting in single (pGL3/ARE1) and double (pGL3/2 × ARE1) insertions. The pGL3/-3046 plasmid containing the 5′-flanking region from −3046 to −1 of the CYP2A6 gene was previously constructed [9]. The pGL3/−1395 and pGL3/−185 plasmids were constructed by ligating the fragments from pGL3/−3046 plasmid digested with BST1107 I/Hind III and Pvu II/Hind III, respectively, into the Sma I/Hind III-digested pGL3-basic plasmid. The pGL3/−1013 plasmid was constructed by ligating the fragments from pGL3/−3046 plasmid digested with Bgl II/Hind III into the Bgl II/Hind III-digested pGL3-basic plasmid. The plasmid DNA was purified by QIAGEN Plasmid Midi kit (QIAGEN). Nucleotide sequences of the constructed plasmids were confirmed by DNA sequencing analyses.

2.6. In vitro transfection and luciferase assay

HepG2 cells were seeded into 24-well plates at 1.0×10^5 cells/well and incubated for 24 h before transfection. Transfection was performed using Tfx-20 reagent (Promega). In brief, the transfection mixture consisted of 150 ng of pGL3 plasmids, 5 ng of phRL-TK plasmid, and 100 ng of Nrf2 expression plasmid (or control vector). Forty-eight hours after the transfection, the cells were harvested and lysed to measure the luciferase activity using a Dual Luciferase Reporter Assay System. The relative luciferase activities were normalized with the Renilla luciferase activities.

2.7. In vivo transfection

Male ICR mice (3 weeks old, 10–13 g) were obtained from SLC Japan (Hamamatsu, Japan). Mice were housed in a controlled environment (temperature 25 ± 1 °C, humidity 50 ± 10%, and 12 h light/12 h dark cycle) in the institutional animal facility with access to food and water ad libitum. Mice were acclimatized for a week before use for the experiments. For in vivo transfection, 18–22 g mice were injected via the tail vein with 10 μg of pGL3 plasmids and 1 μg of pGL4.74 plasmid, in volumes of 0.1 ml/g of body weight within 5–8 s using the TransIT-QR Hydrodynamic Delivery Solution. Endotoxin in plasmid preparations was removed using MiraCLEAN Endotoxin Removal Kit. After 18 h, 1 mg/head SFN or saline was intraperitoneally administered. The dose was decided referring previous studies [19,20]. Animals were sacrificed 24 h later and the liver, approximately 100 mg, was removed and homogenized in 1 ml of passive lysis buffer (Dual Luciferase Reporter Assay System). The liver homogenates were centrifuged at 15,000 rpm for 10 min at 4 °C. Twenty microliters of the supernatant were used to measure the firefly and Renilla luciferase activities. For each construct, at least three mice were transfected, and three independent experiments were performed. Animal maintenance and treatment were conducted in accordance with the National Institutes of Health Guide for Animal Welfare of Japan, as approved by the Institutional Animal Care and Use Committee of Kanazawa University, Japan.

2.8. Statistical analysis

Data are expressed as mean ± SD. Statistical analysis was performed by an unpaired two-tailed Student's t test. A value of P less than 0.05 was considered statistically significant.

3. Results

3.1. SFN induces CYP2A6 mRNA expression in human hepatocytes

We first examined whether the CYP2A6 level in human hepatocytes was increased by SFN treatment (Fig. 1). When human hepatocytes were treated with 10 μM SFN for 12 h, a significant induction (1.4-fold, $P < 0.01$) of the CYP2A6 mRNA level was observed. With 24-h treatment, a similar induction (1.3-fold induction, $P < 0.05$) was observed. These results suggest that CYP2A6 mRNA is induced by SFN.

3.2. Nrf2 directly binds to the ARE on the CYP2A6 gene

To find potential binding sites of Nrf2 on the 5'-flanking region of CYP2A6 gene, we investigated overlapping with the core sequence of consensus ARE 5'-TMAnn<u>RTGAY(C/T)nnnGC</u>Rwwww-3' (core sequence is underlined) using a computer program GENETYX-MAC for all probable nucleotide combination, and thereby we identified three putative AREs up to −4 kb of the 5'-flanking region of CYP2A6 gene. These elements located at −1212, −2444, and −3441 were termed ARE1, ARE2, and ARE3, respectively (Fig. 2). We performed electrophoretic mobility shift assays to examine whether Nrf2 can bind to these AREs (Fig. 3). When the ^{32}P-labeled cARE was incubated with the nuclear extract prepared from the tBHQ-treated HepG2 cells, three bands were detected (Fig. 3, lane 1). The upper and lower bands were non-specific bands (NS). The middle band represented a shifted band, and its density was diminished with both anti-Nrf2 antibodies (C-20) and (H-300) (Fig. 3, lanes 2 and 3).
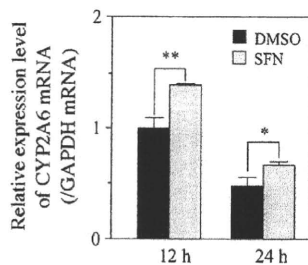

Fig. 3. Electrophoretic mobility shift assays of the binding of Nrf2 to ARE of the CYP2A6 gene. Oligonucleotides of the cARE in Mus musculus HO-1 promoter (left) and CYP2A6 ARE1 (right) were used as probes. Nuclear extracts were prepared from HepG2 cells treated with 80 μM tBHQ for 6 h. Cold oligonucleotides were used as a competitor in 10-, 50-, and 200-fold molar excess. For supershift analyses, 2 μg of anti-Nrf2 antibodies or normal rabbit IgG were preincubated with the nuclear extracts on ice for 30 min.

Super-shifted band was observed only with the anti-Nrf2 antibody (C-20), consistent with our previous study on UGT2B7 [17]. When the ARE1 was used as a probe, a band the mobility of which was the same as that of the cARE–Nrf2 complex was observed (Fig. 3, lane 8). The band was clearly supershifted with the anti-Nrf2 antibody (C-20) (Fig. 3, lane 9) and was competed out by unlabeled cARE (Fig. 3, lanes 12–14). These results indicated that Nrf2 specifically binds to ARE1 on the human CYP2A6 gene. When ARE2 or ARE3 was used as a probe, no band was observed (data not shown).

3.3. ARE1 on CYP2A6 promoter is functional for transactivation via Nrf2

To examine whether ARE1 is functional for the transactivation via Nrf2, luciferase assays were performed using HepG2 cells. We first confirmed that the luciferase activity of the pGL3-cARE plasmid containing two copies of cARE used as a positive control, was significantly ($P < 0.001$) increased up to 2.7-fold by the overexpression of Nrf2 (Fig. 4A). The luciferase activities of the pGL3/ARE1 and pGL3/2 × ARE1 plasmids containing one and two copies of ARE1 were significantly increased up to 1.3- and 2.0-fold, respectively, by the overexpression of Nrf2. Next we performed luciferase assay using a series of reporter plasmids containing the 5'-flanking region of CYP2A6 gene (Fig. 4B). Contrary to our expectations, the luciferase activity of the pGL3/−1013 plasmid containing ARE1 was significantly decreased by the overexpression of Nrf2. The luciferase activities of the pGL3/−1395 and pGL3/−185 plasmids were also significantly decreased by the overexpression of Nrf2. These results suggest that the proximal promoter region possibly has a negative regulatory region responding to Nrf2, or HepG2 cells may lack transcriptional factors crucial for the transcriptional activity of CYP2A6.

3.4. Nrf2 activates CYP2A6 promoter activity in vivo

Next, we sought to determine the transactivity of the plasmids in mice in vivo, because mice liver contains sufficient levels of

Fig. 1. Effects of SFN treatment on the CYP2A6 mRNA level in human hepatocytes. Human hepatocytes were treated with 10 μM SFN or 0.1% DMSO for 12 h or 24 h. Total RNA was extracted and real-time RT-PCR was performed. To normalize the RNA loading, the CYP2A6 mRNA levels were corrected with the GAPDH mRNA levels. Each column represents the mean ± SD of three independent experiments. *$P < 0.05$ and **$P < 0.01$ compared with DMSO treatment.

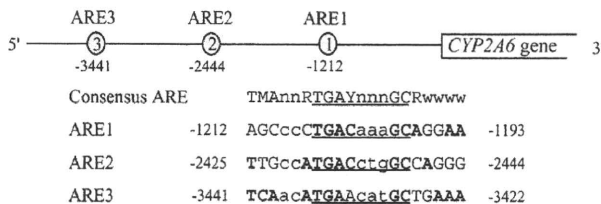|			
Consensus ARE		TMAnn<u>RTGAYnnnGC</u>Rwwww	
ARE1	-1212	AGCcc**CTGAC**aaa**GC**AGG**AA**	-1193
ARE2	-2425	TTGcc**ATGAC**ctg**GC**CAGGG	-2444
ARE3	-3441	**TCA**ac**ATGAA**cat**GC**TGAAA	-3422

Fig. 2. Schematic representation of the putative AREs on the CYP2A6 genes and the sequences of the AREs. Numbers indicate the nucleotide position when the A in the initiation codon ATG is denoted +1 and the base before A is numbered −1. The core ARE sequence is underlined. The nucleotides that are consistent with the consensus ARE are shown with bold letters.
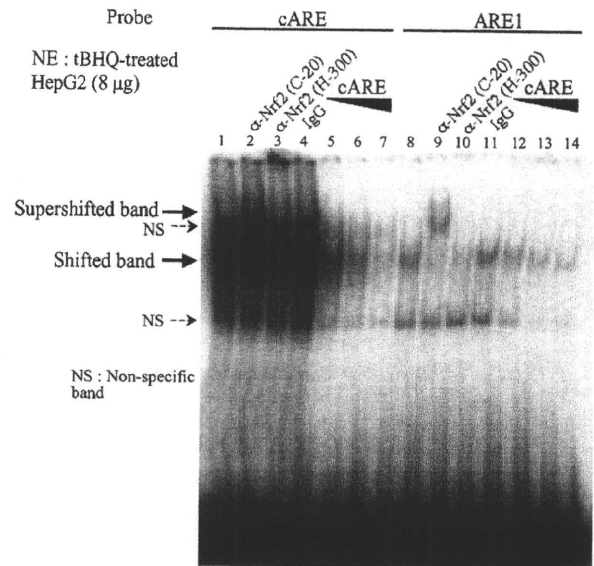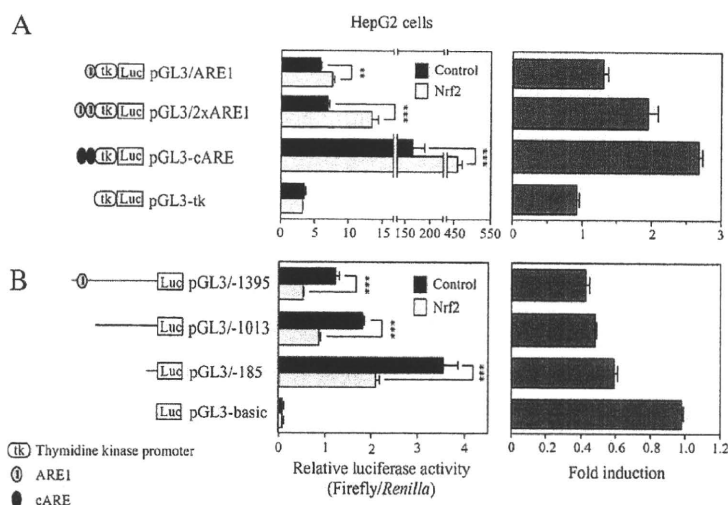
Fig. 4. Effects of overexpression of Nrf2 on CYP2A6 transactivation in HepG2 cells. Reporter plasmids containing ARE sequences (A) or the 5′-flanking region of *CYP2A6* gene with deletion from the 5′ direction (B) were transiently transfected into HepG2 cells with Nrf2 expression plasmid (Nrf2) or pTARGET empty vector (control). The pGL3-cARE plasmid, which contains two copies of the cARE on the human *NQO-1* gene, was used as a positive control. The firefly luciferase activities were normalized with the *Renilla* luciferase activities. Right panel shows the fold induction of the transcriptional activity by the overexpression of Nrf2. Each column represents the mean ± SD of three independent experiments. **$P < 0.01$ and ***$P < 0.001$ compared with control.

hepatic transcription factors, which is unlikely the case in cell lines. When the pGL3-cARE plasmid was injected into mice, the luciferase activity in the liver was significantly ($P < 0.05$) increased up to 2.1-fold by SFN treatment (Fig. 5A). It was confirmed that under this condition the endogenous mouse NQO1 mRNA level was significantly ($P < 0.001$) induced (2.4-fold) (Fig. 5B). The luciferase activity of the pGL3/−1395 plasmid containing ARE1 was significantly ($P < 0.05$) increased (1.9-fold) by SFN treatment, but that of the pGL3/−1013 plasmid was not (Fig. 5A). These results suggest that the CYP2A6 promoter containing ARE1 is transactivated by SFN in vivo.

4. Discussion

In the present study, we found that Nrf2 is involved in the regulation of human CYP2A6. Concerning the role of Nrf2 in the regulation of P450, mouse Cyp2a5 was the first reported case [12]. In addition, a recent study demonstrated that human CYP2J2 is regulated by Nrf2 [21]. We could provide evidence to put CYP2A6 into the short list of P450 s that are regulated by Nrf2. It was clearly demonstrated that sulforaphane significantly increased the CYP2A6 mRNA level in human hepatocytes. Sulforaphane, an activator of Nrf2, is contained in cruciferous vegetables such as broccoli sprouts,
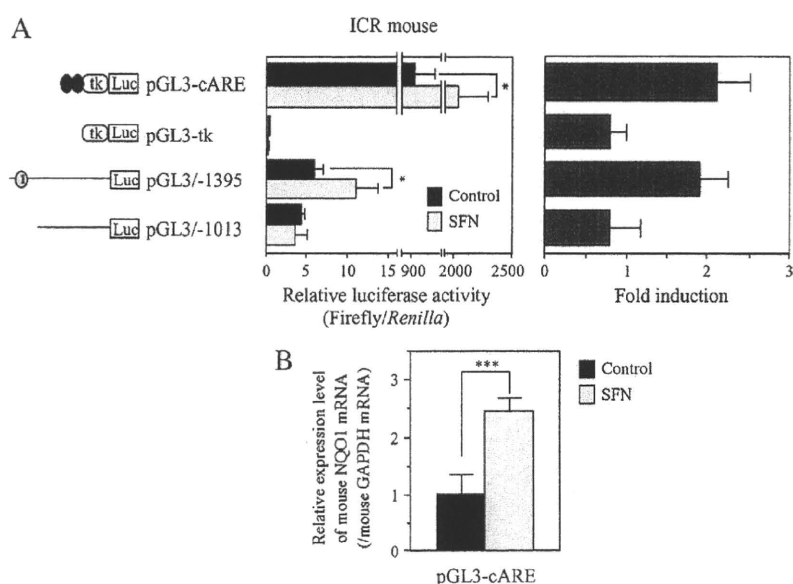

Fig. 5. Effects of SFN on CYP2A6 transactivation in in vivo mice liver transfections. Ten μg of pGL3 reporter plasmid and 1 μg of pGL4.74 plasmid were injected into the tail vein of male ICR mice. After 18 h, 1 mg/head SFN was intraperitoneally administered. After 6 h, the liver was removed and the homogenate and total RNA were prepared for the luciferase assay and real-time RT-PCR, respectively. (A) The firefly luciferase activities were normalized with the *Renilla* luciferase activities. Right panel shows the fold induction of the transcriptional activity by the treatment with SFN. Each column represents the mean ± SD (n = 3). *$P < 0.05$ compared with control. (B) NQO1 mRNA levels in mice injected with pGL3-cARE plasmid were determined by real-time RT-PCR. The NQO1 mRNA levels were normalized with the GAPDH mRNA levels. Each column represents the mean ± SD (n = 3). ***$P < 0.001$ compared with saline.

horseradish, cabbage, and watercress. Interestingly, it has been reported that CYP2A6 activities were significantly increased after the consumption broccoli (500 g/day for 6 days) by 1.4- to 5.5-fold [14]. We believe that the present study may demonstrate the underlying molecular mechanism of the induction.

Electrophoretic mobility shift assays clearly demonstrated that Nrf2 directly bound to ARE1, but not ARE2 and ARE3, on the human CYP2A6 gene. Previously, Abu-Bakar et al. [22] identified ARE (TGACagaGCA) at −2377 on the 5′-flanking region of the mouse Cyp2a5 gene to which Nrf2 bound. Interestingly, the sequence of human ARE1 (TGACaaaGCA) has only one base difference with the mouse ARE. Although the core sequence of ARE2 (TGACctgGCc) is similar to that of ARE1, Nrf2 did not bind to ARE2. Thus, the differences in core sequence (underlined) might also be important for the binding of Nrf2. For the supershift assay, we used two kinds of anti-Nrf2 antibody (C-20 and H-300). The supershifted band was observed with the anti-Nrf2 antibody (C-20) but not with the anti-Nrf2 antibody (H-300). Anti-Nrf2 antibody (C-20) recognizes the C-terminal of Nrf2, whereas anti-Nrf2 antibody (H-300) recognizes the N-terminal. Since the N-terminal has a DNA-binding domain, the anti-Nrf2 antibody (H-300) seemed to interfere with the binding of Nrf2 to the DNA, not forming the antibody-Nrf2-DNA complex represented as a supershifted band.

In the luciferase assays, we first determined the effects of the treatment with SFN on the transactivity of the constructs. Unexpectedly, SFN treatment significantly decreased the firefly and Renilla luciferase activities derived from the pGL3-tk and phRL-TK plasmids, respectively by approximately half (data not shown). Such a phenomenon was not observed when Nrf2 was over-expressed. It was assumed that SFN might affect the thymidine kinase promoter activities independently of Nrf2. By the over-expression of Nrf2, we found that ARE1 itself was functional for the transactivation. However, the luciferase activities of plasmids containing the intact 5′-flanking region of CYP2A6 gene were not increased by the overexpression of Nrf2, even if it contained the ARE1. Similar results were obtained using HeLa cells (data not shown), suggesting that it was not a HepG2-specific phenomenon. It was considered that the sequences surrounding ARE may interfere the binding of Nr2, or these cell lines might lack some transcriptional factor(s) that are necessary for the transactivation of CYP2A6. It has been reported that the transactivity of the CYP2C8 promoter was successfully evaluated by the injection of the constructs in mouse in vivo, although such evaluation was unsuccessful in HepG2 cells [23]. Based on this report, we also performed the luciferase assay in mice in vivo and found that the SFN treatment significantly increased the transactivity of the pGL3/−1395 plasmid containing ARE1 (Fig. 5A). Thus, it was concluded that CYP2A6 is regulated by Nrf2 via ARE1.

CYP2A6 is responsible for nicotine metabolism [2]. Smokers adapt their smoking behavior to maintain their nicotine levels in the body [24]. Since the metabolism of nicotine by CYP2A6 is the principal pathway by which nicotine is removed from the circulation, an association between the CYP2A6 activity and cigarette consumption has been suggested [5,6]. Cigarette smoking is known to cause oxidative stress, which activates Nrf2 [25,26]. In addition, tobacco is a substantial source of cadmium, supported by the fact that the serum cadmium level of smokers is 3-folds higher than that of non-smokers [27]. Therefore, it is surmised that the CYP2A6 expression level might be higher in smokers than in non-smokers, although there is no report comparing the expression level of hepatic CYP2A6 protein in smokers versus that in non-smokers. In contrast, it has been reported that in vivo nicotine clearance [28] and in vivo coumarin metabolism [29] were lower in smokers than in non-smokers, suggesting the possibility that some constituents in tobacco smoke might have inhibitory effects on the

CYP2A6 activity. Such inhibitory effects could possibly mask the induction of CYP2A6, resulting in decreased in vivo metabolic potency. Thus, it would be of interest to compare the hepatic CYP2A6 expression levels in smokers and non-smokers, although it has been reported that the administration of nicotine itself downregulated CYP2A6-like enzyme expression in African green monkeys [30].

In conclusion, we found that Nrf2 regulates the human CYP2A6. This mechanism implies the possibility that the CYP2A6 expression may be increased by oxidative stress such as by cigarette smoking.

Acknowledgements

References

[1] Yun CH, Shimada T, Guengerich FP. Purification and characterization of human liver microsomal cytochrome P-450 2A6. Mol Pharmacol 1991;40:679–85.

[2] Nakajima M, Yamamoto T, Nunoya K, Yokoi T, Nagashima K, Inoue K, et al. Role of human cytochrome P4502A6 in C-oxidation of nicotine. Drug Metab Dispos 1996;24:1212–7.

[3] Nakajima M, Yamamoto T, Nunoya K, Yokoi T, Nagashima K, Inoue K, et al. Characterization of CYP2A6 involved in 3′-hydroxylation of cotinine in human liver microsomes. J Pharmacol Exp Ther 1996;277:1010–5.

[4] Tiano HF, Hosokawa M, Chulada PC, Smith PB, Wang RL, Gonzalez FJ, et al. Retroviral mediated expression of human cytochrome P450 2A6 in C3H/10T1/2 cells confers transformability by 4-(methylnitrosamino)-1-(3-pyridyl)-1-butanone (NNK). Carcinogenesis 1993;14:1421–7.

[5] Nakajima M. Smoking behavior and related cancers: the role of CYP2A6 polymorphisms. Curr Opin Mol Ther 2007;9:538–44.

[6] Strasser AA, Malaiyandi V, Hoffmann E, Tyndale RF, Lerman C. An association of CYP2A6 genotype and smoking topography. Nicotine Tob Res 2007;9:511–8.

[7] Fujieda M, Yamazaki H, Saito T, Kiyotani K, Gyamfi MA, Sakurai M, et al. Evaluation of CYP2A6 genetic polymorphisms as determinants of smoking behavior and tobacco-related lung cancer risk in male Japanese smokers. Carcinogenesis 2004;25:2451–8.

[8] Itoh M, Nakajima M, Higashi E, Yoshida R, Nagata K, Yamazoe Y, et al. Induction of human CYP2A6 is mediated by the pregnane X receptor with peroxisome proliferator-activated receptor-γ coactivator 1α. J Pharmacol Exp Ther 2006;319:693–702.

[9] Higashi E, Fukami T, Itoh M, Kyo S, Inoue M, Yokoi T, et al. Human CYP2A6 is induced by estrogen via estrogen receptor. Drug Metab Dispos 2007;35:1935–41.

[10] Onica T, Nichols K, Larin M, Ng L, Maslen A, Dvorak Z, et al. Dexamethasone-mediated up-regulation of human CYP2A6 involves the glucocorticoid receptor and increased binding of hepatic nuclear factor 4 alpha to the proximal promoter. Mol Pharmacol 2008;73:451–60.

[11] Satarug S, Nishijo M, Ujjin P, Vanavanitkun Y, Baker JR, Moore MR. Effects of chronic exposure to low-level cadmium on renal tubular function and CYP2A6-mediated coumarin metabolism in healthy human subjects. Toxicol Lett 2004;148:187–97.

[12] Abu-Bakar A, Satarug S, Marks GC, Lang MA, Moore MR. Acute cadmium chloride administration induces hepatic and renal CYP2A5 mRNA, protein and activity in the mouse: involvement of transcription factor NRF2. Toxicol Lett 2004;148:199–210.

[13] Itoh K, Chiba T, Takahashi S, Ishii T, Igarashi K, Katoh Y, et al. An Nrf2/small Maf heterodimer mediates the induction of phase II detoxifying enzyme genes through antioxidant response elements. Biochem Biophys Res Commun 1997;236:313–22.

[14] Hakooz N, Hamdan I. Effects of dietary broccoli on human in vivo caffeine metabolism: a pilot study on a group of Jordanian volunteers. Curr Drug Metab 2007;8:9–15.

[15] Nakajima M, Itoh M, Sakai H, Fukami T, Katoh M, Yamazaki H, et al. CYP2A13 expressed in human bladder metabolically activates 4-aminobiphenyl. Int J Cancer 2006;119:2520–6.

[16] Tsuchiya Y, Nakajima M, Kyo S, Kanaya T, Inoue M, Yokoi T. Human CYP1B1 is regulated by estradiol via estrogen receptor. Cancer Res 2004;64:3119–25.

[17] Nakamura A, Nakajima M, Higashi E, Yamanaka H, Yokoi T. Genetic polymorphisms in the 5′-flanking region of human UDP-glucuronosyltransferase 2B7 affect the Nrf2-dependent transcriptional regulation. Pharmacogenet Genomics 2008;18:709–20.

[18] Balogun E, Hoque M, Gong P, Killeen E, Green CJ, Foresti R, et al. Curcumin activates the haem oxygenase-1 gene via regulation of Nrf2 and the antioxidant-responsive element. Biochem J 2003;371:887–95.

[19] Innamorato NG, Rojo AI, García-Yagüe AJ, Yamamoto M, de Ceballos ML, Cuadrado A. The transcription factor Nrf2 is a therapeutic target against brain inflammation. J Immunol 2008;181:680–9.

[20] Kong L, Tanito M, Huang Z, Li F, Zhou X, Zaharia A, et al. Delay of photoreceptor degeneration in tubby mouse by sulforaphane. J Neurochem 2007;101:1041–52.

[21] Lee AC, Murray M. Up-regulation of human CYP2J2 in HepG2 cells by butylated hydroxyanisole is mediated by c-Jun and Nrf2. Mol Pharmacol 2010;77:987–94.

[22] Abu-Bakar A, Lämsä V, Arpiainen S, Moore MR, Lang MA, Hakkola J. Regulation of CYP2A5 gene by the transcription factor nuclear factor (erythroid-derived 2)-like 2. Drug Metab Dispos 2007;35:787–94.

[23] Rodríguez-Antona C, Niemi M, Backman JT, Kajosaari LI, Neuvonen PJ, Robledo M, et al. Characterization of novel CYP2C8 haplotypes and their contribution to paclitaxel and repaglinide metabolism. Pharmacogenomics J 2008;8:268–77.

[24] Benowitz NL. Pharmacology of nicotine: addiction and therapeutics. Annu Rev Pharmacol Toxicol 1996;36:597–613.

[25] Hübner RH, Schwartz JD, De Bishnu P, Ferris B, Omberg L, Mezey JG, et al. Coordinate control of expression of Nrf2-modulated genes in the human small airway epithelium is highly responsive to cigarette smoking. Mol Med 2009;15:203–19.

[26] Boutten A, Goven D, Boczkowski J, Bonay M. Oxidative stress targets in pulmonary emphysema: focus on the Nrf2 pathway. Expert Opin Ther Targets 2010;14:329–46.

[27] Anetor JI, Ajose F, Anetor GO, Iyanda AA, Babalola OO, Adeniyi FA. High cadmium/zinc ratio in cigarette smokers: potential implications as a biomarker of risk of prostate cancer. Niger J Physiol Sci 2008;23:41–9.

[28] Benowitz NL, Jacob III P. Nicotine and cotinine elimination pharmacokinetics in smokers and nonsmokers. Clin Pharmacol Ther 1993;53:316–23.

[29] Poland RE, Pechnick RN, Cloak CC, Wan YJ, Nuccio I, Lin KM. Effect of cigarette smoking on coumarin metabolism in humans. Nicotine Tob Res 2000;2:351–4.

[30] Schoedel KA, Sellers EM, Palmour R, Tyndale RF. Down-regulation of hepatic nicotine metabolism and a CYP2A6-like enzyme in African green monkeys after long-term nicotine administration. Mol Pharmacol 2003;63:96–104.

Toxicological Evaluation of Acyl Glucuronides of Nonsteroidal Anti-Inflammatory Drugs Using Human Embryonic Kidney 293 Cells Stably Expressing Human UDP-Glucuronosyltransferase and Human Hepatocytes[S]

Toshihisa Koga, Ryoichi Fujiwara, Miki Nakajima, and Tsuyoshi Yokoi

Drug Metabolism and Toxicology, Faculty of Pharmaceutical Sciences, Kanazawa University, Kanazawa, Japan

ABSTRACT:

The chemical reactivity of acyl glucuronide (AG) has been thought to be associated with the toxic properties of drugs containing carboxylic acid moieties, but there has been no direct evidence that AG formation was related to the toxicity. In the present study, the cytotoxicity and genotoxicity of AGs were investigated. Human embryonic kidney (HEK) 293 cells stably expressing UDP-glucuronosyltransferase (UGT) 1A3 (HEK/UGT1A3) were constructed to assess the cytotoxicity of AGs, and HEK/UGT1A4 cells were also used as a negative reference. After exposure to nonsteroidal anti-inflammatory drugs (NSAIDs) such as naproxen (1 mM), diclofenac (0.1 mM), ketoprofen (1 mM), or ibuprofen (1 mM) for 24 h, HEK/UGT1A3 cells produced AG in a time-dependent manner. However, HEK/UGT1A4 cells hardly produced AG. The cytotoxicity of HEK/ UGT1A3 cells was not increased compared with that of HEK/ UGT1A4 cells. In addition, the AG formed in NSAID-treated human hepatocytes was decreased from one-third to one-ninth by treatment with (−)-borneol, an inhibitor of acyl glucuronidation, but the cytotoxicity was increased. These results indicated that AG formation reflected the detoxification process in human hepatocytes. Furthermore, the possibility of genotoxicity from the AG formed in NSAID-treated HEK/UGT cells was investigated by the comet assay, and DNA damage was not detected in any HEK/UGT cell lines. In conclusion, the in vitro cytotoxic and genotoxic effects of the AGs of NSAIDs were investigated and AG was not found to be a causal factor in the toxicity.

Introduction

Some of the most commonly prescribed medications and over-the-counter drugs are carboxylate compounds, including many nonsteroidal anti-inflammatory drugs (NSAIDs) and fibrate lipid-lowering drugs. Approximately 25% of drugs withdrawn from the market around the world because of severe toxicity have been carboxylic acids, such as the NSAIDs ibufenac, zomepirac, bromfenac, suprofen, and benoxaprofen. Among drugs containing carboxylic acid, NSAIDs are associated with some degree of hepatotoxicity, immune cytopenias, and hypersensitivity reactions (Bailey and Dickinson, 2003). However, the essential cause of the toxicity is uncertain because of the structural diversity of NSAIDs. For example, diclofenac is associated with hepatotoxicity with a low incidence of 6 to 18 cases/100,000 person-years (Walker, 1997). Both immunological and nonimmunological mechanisms have been proposed to be responsible for the diclofenac hepatotoxicity (Banks et al., 1995; Wade et al., 1997).

Glucuronidation is one of the most important phase II metabolic pathways for endogenous and exogenous substrates in humans. Because glucuronides usually possess less intrinsic biological or chemical activity than their parent aglycones and are rapidly excreted, glucuronidation is considered to be a detoxification reaction (Shipkova et al., 2003). However, acyl glucuronide (AG), which is characterized by its electrophilic reactivity, has been implicated in a wide range of adverse drug effects including drug hypersensitivity reactions and cellular toxicity (Ritter, 2000). It is well known that AG is unstable in physiological conditions and consequently undergoes hydrolysis or intramolecular rearrangement, which occurs by migration of the drug moiety from the 1-O-β position to 2-, 3-, and 4-positions on the glucuronic acid ring (Bailey and Dickinson, 2003; Shipkova et al., 2003). As a result, AG potentially binds to cellular macromolecules covalently and has been suspected to mediate idiosyncratic drug toxicities associated with carboxylic drugs (Boelsterli et al., 1995).

ABBREVIATIONS: NSAID, nonsteroidal anti-inflammatory drug; AG, acyl glucuronide; UGT, UDP-glucuronosyltransferase; HEK, human embryonic kidney; DMSO, dimethyl sulfoxide; UDPGA, UDP-glucuronic acid; 4-MU, 4-methylumbelliferone; GAPDH, glyceraldehyde-3-phosphate dehydrogenase; PAGE, polyacrylamide gel electrophoresis; PBS, phosphate-buffered saline; HPLC, high-performance liquid chromatography; FBS, fetal bovine serum; DMEM, Dulbecco's modified Eagle's medium; LC, liquid chromatography; MS/MS, tandem mass spectrometry; MTT, 3-(4,5-dimethylthiazol-2-yl)-2,5-diphenyltetrazolium; WST-8, 2-(2-methoxy-4-nitrophenyl)-3-(4-nitrophenyl)-5-(2, 4-disulfophenyl)-2H-tetrazolium monosodium salt; LDH, lactic dehydrogenase.